

# Liquid Metal Electrodes for Energy Storage Batteries

Haomiao Li, Huayi Yin, Kangli Wang,\* Shijie Cheng, Kai Jiang,\* and Donald R. Sadoway

The increasing demands for integration of renewable energy into the grid and urgently needed devices for peak shaving and power rating of the grid both call for low-cost and large-scale energy storage technologies. The use of secondary batteries is considered one of the most effective approaches to solving the intermittency of renewables and smoothing the power fluctuations of the grid. In these batteries, the states of the electrode highly affect the performance and manufacturing process of the battery, and therefore leverage the price of the battery. A battery with liquid metal electrodes is easy to scale up and has a low cost and long cycle life. In this progress report, the state-of-the-art overview of liquid metal electrodes (LMEs) in batteries is reviewed, including the LMEs in liquid metal batteries (LMBs) and the liquid sodium electrode in sodium-sulfur (Na-S) and ZEBRA (Na-NiCl<sub>2</sub>) batteries. Besides the LMEs, the development of electrolytes for LMEs and the challenge of using LMEs in the batteries, and the future prospects of using LMEs are also discussed.

## 1. Introduction

With increasing concern for energy and environmental issues, renewable energy, such as wind and solar, will play a more and more important role in reducing greenhouse gas emissions and thereby achieving the global sustainability. The introduction of more renewable energy into the grid urgently calls for large-scale energy storage technologies (ESTs). For example, the integration of large-scale wind or/and solar power into the grid needs ESTs to tackle the intrinsic intermittency and fluctuation of renewables.<sup>[1]</sup> Moreover, ESTs are very important for peak shaving and power rating for all the stages of generation, transmission, distribution and end user in the smart grid. Therefore, the low-cost, long-lasting and high-efficiency ESTs are key enablers for the increasing renewable energy and smart grid applications.

H. M. Li, Dr. K. L. Wang, Prof. S. J. Cheng, Prof. K. Jiang  
State Key Laboratory of Advanced Electromagnetic  
Engineering and Technology  
School of Electrical and Electronic Engineering  
State Key Laboratory of Materials Processing  
and Die & Mould Technology  
College of Materials Science and Engineering  
Huazhong University of Science and Technology  
Wuhan, Hubei 430074, China  
E-mail: klwang@hust.edu.cn; kjiang@hust.edu.cn

Dr. H. Y. Yin, Prof. D. R. Sadoway  
Department of Materials Science and Engineering  
Massachusetts Institute of Technology  
77 Massachusetts Avenue, Cambridge, Massachusetts 02139-4307, USA



DOI: 10.1002/aenm.201600483

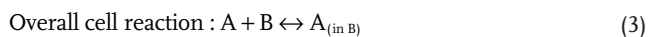
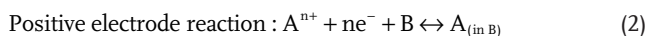
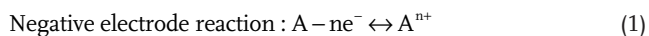
Rechargeable batteries are considered one of the most promising energy storage technologies thanks to the desirable features of flexibility, high efficiency and long cycle life.<sup>[2]</sup> A battery commonly consists of anode, cathode and electrolyte, and the electrolyte is sandwiched between the cathode and anode, shuttling ions between the two electrodes. Different kinds of batteries have their own applications in different fields, e.g., portable devices, electrical vehicles and grid energy storage. The major existing energy storage battery technologies, such as sodium-sulfur batteries, redox-flow batteries and lithium ion batteries, have been demonstrated for up to MW-level grid applications. Besides these batteries, many new types of batteries are being researched aiming

at developing low cost and long lifetime technologies for large-scale energy storage.<sup>[3-8]</sup> As shown in **Table 1**, the states of the electrode in typical batteries are solid and liquid with the possibility of gas state, and the states of the electrolyte are liquid and solid. Batteries with liquid metal electrodes (LMEs) are easy to scale up, usually have low cost and long cycle life, thanks to the conductive and amorphous liquid metal electrode structure. There are typically two types of batteries employing liquid metal electrodes: (1) Na-beta alumina batteries, including Na-S and ZEBRA batteries with liquid Na anode; (2) liquid metal batteries (LMBs) with both liquid metal anode and cathode. Besides the application in energy storage batteries, LMEs had attracted much attention in electrolysis (e.g., aluminum electrolysis cell) and electroanalytical chemistry (e.g., dropping mercury electrode).

### 1.1. Liquid Metal Electrode-Based Batteries

The typical battery employing LMEs is the liquid metal battery (LMB). As shown in **Figure 1**, a LMB is composed of three liquid layers: a molten salt layer in the middle and two liquid metal layers sitting at the top and bottom. The two liquid metal layers behave as negative and positive electrodes, and the molten salt layer serves as electrolyte and separator; all of the components are self-segregated into three layers due to their different densities and mutual immiscibility. The electrochemical processes of LMB are driven by the different electronegativity of the two liquid metal layers. In the discharge process, the negative electrode (lighter metal/alloy at the top), metal A, is oxidized to A<sup>++</sup> which subsequently dissolves in the molten salt electrolyte and then alloys with the liquid metal B, the positive electrode (heavier metal/alloy at bottom). In the charge process, A<sub>(in B)</sub>

is oxidized to  $A^{n+}$  at the positive electrode/electrolyte interface, and the  $A^{n+}$  is reduced back to  $A$  at the negative electrode, which is called the dealloying process. The electrode and overall cell reactions are expressed in Equations (1–3).



LMEs can be widely found in the electrochemical cells for producing liquid metals (Li, Na, Mg, Al, etc.) via molten salt electrolysis. A huge amount of electricity is currently consumed in industry by electrolysis, like the Hall–Héroult process for aluminum production.<sup>[12,13]</sup> Conversely, the electrolysis cell can store huge electric energy if the electrolysis process can be reversed. This is the original idea of inventing LMBs for large-scale energy storage. By replacing the carbon anode with a liquid metal in the molten salt electrolysis cell, the first LMB with both liquid anode and cathode was developed by Sadoway et al.<sup>[14]</sup> According to the basic physicochemical properties of the metals, the possible candidate metals for use as electrodes for LMEs must have low melting point. In addition to the temperature, the cost is also a key criterion for selecting materials for LMBs. **Figure 2** shows the price and melting point of the metals of melting temperature under 1000 °C.

Owing to the three-liquid-layer structure, LMB has the following advantages for larger-scale grid energy storage: (1) low cost due to the use of cheap inorganic materials; (2) high rate and long lifespan due to the fast kinetics of liquid electrodes with no dendrite formation and/or electrode materials deformation; (3) easy assembling and scale-up due to the self-assembling process without conventional membrane. Based on the above-mentioned merits of LMBs, a start-up called Ambri (formerly named Liquid Metal Battery Corporation),<sup>[15]</sup> is developing and commercializing this new technology. At Ambri, 20 kWh LMB core cells have been tested and a MW level system has been conceived, which preliminarily proved the concept of LMB for large-scale grid application. However, as an emerging EST, the development of LMB still faces some challenges on both materials and engineering, which will be discussed later in this review paper.

Another type of batteries employing liquid metal electrodes are sodium-beta alumina batteries including Na–S and ZEBRA batteries, which both have a liquid sodium anode with a  $\text{Na}^+$  selective ceramic conductor,  $\beta/\beta'$ -alumina, as the solid-state electrolyte. Owing to the increasing cost of lithium resources and the high cost of lithium ion batteries (LIBs), sodium based batteries are now being considered as one of the most promising electrochemical systems for grid energy storage.<sup>[16]</sup> Moreover, Na is a low-cost, environmentally benign and earth-abundant element, which spurs the study of Na-based batteries. As the reduction potential of sodium is only 0.3 V less negative than lithium ( $E^\circ_{(\text{Na}^+/\text{Na})} = -2.71 \text{ V vs SHE}$ ), the open circuit voltage (OCV) of the battery with a Na electrode is only 0.3 V less than a Li-based battery when the same cathode is applied. Albeit having a less negative reduction potential than lithium, sodium



**Kangli Wang** received her Ph.D. in electrochemistry from Wuhan University, China in 2006. From 2007 to 2010, she was a postdoctoral fellow in the group of Professor Jeffrey Fergus in Material Engineering at Auburn University. From 2010 to 2013, she was a postdoctoral associate in Professor Donald Sadoway's group at MIT.

She is currently a Chutian Scholar associate professor at School of Electrical and Electronic Engineering in HUST. Her research interests mainly focus on energy storage technologies and advanced energy materials.



**Kai Jiang** received his BSc (1999) in physical chemistry and Ph.D. (2006) in electrochemistry at Wuhan University, China. He was a visiting scholar at Auburn University between 2007 and 2009. Prior to joining HUST, Prof. Jiang worked as a postdoctoral associate in the Department of Materials Science and Engineering at

MIT. Currently, he is a professor at HUST in China. His current research interests focus on electrochemical energy storage technologies and advanced materials for sustainable energy.



**Donald Sadoway** is the John F. Elliott Professor of Materials Chemistry in the Department of Materials Science and Engineering at MIT. His research into the electrochemistry of molten salts has resulted in the invention of a rechargeable battery for grid-level storage applications and the development of environmentally

sound electrochemical technology for the extraction, refining, and recycling of metals. Sadoway obtained a BSc. in Engineering Science, a MSc, and a Ph.D. in Chemical Metallurgy, all from the University of Toronto.

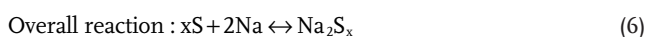
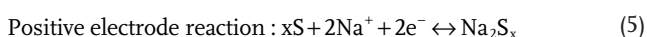
is less reactive than Li, allowing the ease of selecting secondary battery materials and separator. For example, Na is compatible with  $\text{Al}_2\text{O}_3$  which is a commonly used ceramic. Since the invention of  $\beta'$ - $\text{Al}_2\text{O}_3$ , Na–S and ZEBRA batteries with molten Na anode have been developed.<sup>[12]</sup> The half and overall reactions of the Na–S and ZEBRA batteries are as follows:

**Table 1.** States of the anode, cathode and electrolyte in the typical batteries. S, L and G refer to solid, liquid and gas states.<sup>[2,9–11]</sup>

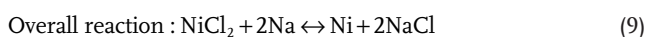
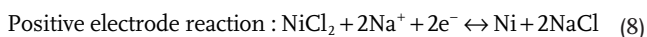
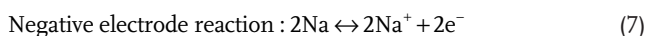
Batteries	State <sup>a)</sup>	Lifetime [cycle]	Cost [\$ kWh <sup>-1</sup> ]	Energy density [Wh kg <sup>-1</sup> ]	System scale
Li-ion	S   L(S)   S	4500	500–1420	75–200	MW
Na-ion	S   L(S)   S	–	–	–	–
Lead acid	S   L   S	≈1000	200–400	30–50	MW
Ni–Cd	S   L   S	2000	800–1500	≈50	–
Ni–MH	S   L   S	2000	–	50–70	–
Li–air	S   L(S)   G	–	300–700	500–1000	–
Flow <sup>b)</sup>	L(S)   S   L	>10000	750–830	10–30	MW
Na–S	L   S   L	4500	400–555	120–240	MW
ZEBRA	L   S   L	3000	400–900	90–120	MW
LMB <sup>c)</sup>	L   L   L	>10000	< 150	50–200	–

<sup>a)</sup>S, L and G refer to solid, liquid and gas states in cell of anode | electrolyte | cathode. <sup>b)</sup>The cost calculated based on all V redox system. <sup>c)</sup>The cost calculated based on electrode and electrolyte materials in LMBs.

### Na–S battery



### ZEBRA battery



As shown in **Figure 3**, Na–S and ZEBRA batteries have the same liquid Na anode contacting with tubular  $\beta''\text{-Al}_2\text{O}_3$  electrolyte; the Na–S cell has the liquid sulfur cathode; and the ZEBRA cell has a solid porous  $\text{NiCl}_2$  cathode and a secondary  $\text{NaCl-AlCl}_3$  electrolyte. The OCV of Na–S cell is between 1.78 and 2.08 V at the operating temperature of  $\approx 350$  °C, and the OCV of ZEBRA battery is 2.58 V at 300 °C.

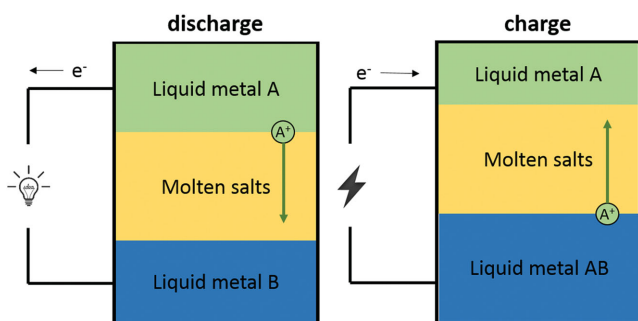


**Figure 1.** Schematic of liquid metal battery in the discharge and charge processes.

## 1.2. Advantages and Disadvantages of Liquid Metal Electrodes

Metal electrodes are most widely used in batteries, and they are usually in the form of solid and liquid states. Compared with solid metal electrodes (SMEs), LMEs possess the following merits: (1) no dendrite formation during electrodeposition process; (2) no phase deformation or grain size change during charge/discharge; (3) ease of building stable electrode/electrolyte interfaces and fabricating cells. As shown in **Figure 4**, electrochemical process on SMEs can result in dendrite formation and structure collapsed. However, batteries with LMEs avoid such deleterious electrode processes and thereby are safely operating for long service lifetimes due to the self-healing function of the liquidity of the LMEs. Besides, it has been recognized that the state of the electrodes is highly related to the manufacturing process of the battery, and therefore largely affects capability for scale-up and the cost of batteries. For example, the flow battery with liquid electrodes is easier to scale up than lithium ion batteries with solid electrodes. The simple manufacturing process and excellent scalability of liquid-electrode-based batteries show great potential for large-scale energy storage application. However, most LMEs only work at high operating temperature ( $> 200$  °C) and consequently the full batteries containing LMEs should be operating at a high temperature, too. A high operating temperature corresponds to high vapor pressure of liquid metals and electrolytes, high cost of the secondary battery materials, and a more obvious corrosion issues. Moreover, a long-term hermetic seal at high temperature is difficult to build because most of the polymeric seals usually cannot survive over 200 °C.

**Table 2** shows the properties of some typical liquid metals (lithium, sodium, potassium, calcium and magnesium) used as negative electrodes for LME-based batteries. In this review, we will mainly focus on the recent development of the LMEs for LMBs and Na-beta alumina batteries.

## 2. Lithium-Based Liquid Electrode

Lithium (Li) is the lightest metal and has the lowest oxidation potential among all elements ( $< -3$  V vs standard hydrogen

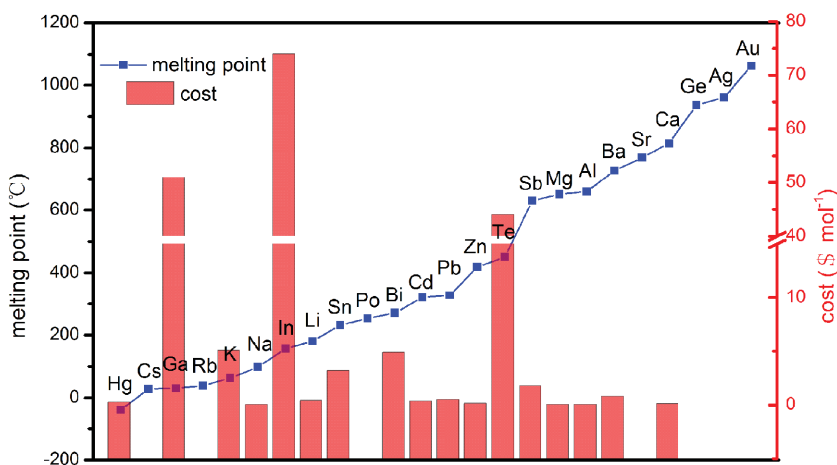


Figure 2. The costs and melting points of the metals under 1000 °C.

potential). Therefore, lithium batteries have high energy and power densities, like the well-known LIBs.<sup>[36]</sup> Although Li is an attractive metal electrode, it is still hard to employ solid lithium in secondary batteries because of formation of dendrite Li during the cycling. Efforts for solving the problem by cur-tailing dendrite growth are key to the success of using pure Li metal in batteries. One approach is to optimize the electrolyte and/or modify the surface of current collector to suppress the dendrite growth.<sup>[37]</sup> Another way is to use liquid Li electrode at elevated temperature. The relatively low melting point of Li at 180 °C makes it easy to be a liquid state just above 180 °C, for example, the liquid Li anode in LMBs. However, most of the commonly used organic electrolytes are not stable at such high temperature, and the formation of SEI is still hard to prevent the Li metal from reacting with the organic electrolyte. In this regard, molten salts, especially the liquid halide salts, are compatible with the liquid Li electrode and have been employed in the high temperature batteries.<sup>[38,39]</sup> To ensure the high Li<sup>+</sup> conductivity, lithium-based molten halide salts (LiF, LiCl, LiBr and LiI) with high ionic conductivity (1.75–3.5 S cm<sup>-1</sup>) and low

melting point have been widely employed in molten salts based batteries.<sup>[40]</sup> Besides the relatively low melting point and high ionic conductivity of molten salts, lithium has low solubility in Li-based molten electrolytes (0.5–2.5% in molar, same below), allowing the batteries to have high Coulombic efficiency of the batteries. In 1960s, lithium-based bimetallic cells were studied, and the Li–Te cell was demonstrated aiming at electric vehicle applications. Later, the attention was shifted to higher energy density systems such as Li–FeS/FeS<sub>2</sub>,<sup>[41,42]</sup> while the relatively low specific energy bimetallic galvanic cells were ignored in the next few decades because of their limitations for portable applications. As the recently increasing demand for grid energy storage devices, lithium-based bime-

talic batteries re-attracted researchers' attention about 50 years later with the concept of liquid metal battery (LMB) being put forward. In this section, the application of liquid Li electrode in LMBs will be reviewed.

### 2.1. Lithium (Li) – Tellurium (Te) System

Tellurium is one of the most electronegative elements among all candidate positive metal electrode materials for LMBs, and the OCV of lithium-tellurium system is 1.75 V.<sup>[27,43]</sup> Due to the high OCV, Li–Te was initially attempted to be researched as high energy density batteries. H. Shimotake et al.<sup>[20]</sup> firstly employed liquid Li and Te as negative and positive electrodes, respectively, and LiF–LiCl–LiI as electrolyte assembling a cell operating at 480 °C. The cell showed good rate capability and cyclability (Figure 5). In order to confine the molten electrolyte in between the two liquid electrodes, a paste electrolyte was employed in the cells for safety. The paste electrolyte is a mixture of molten salt and inert filler materials (such as ceramic

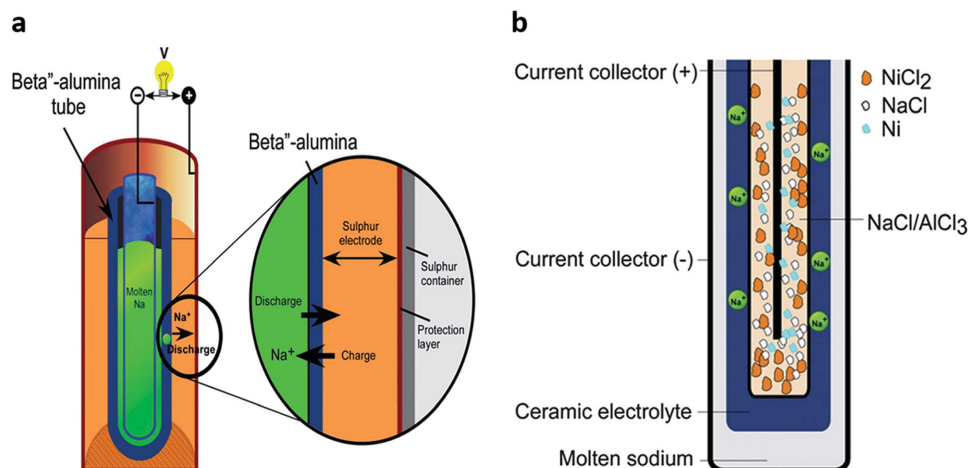
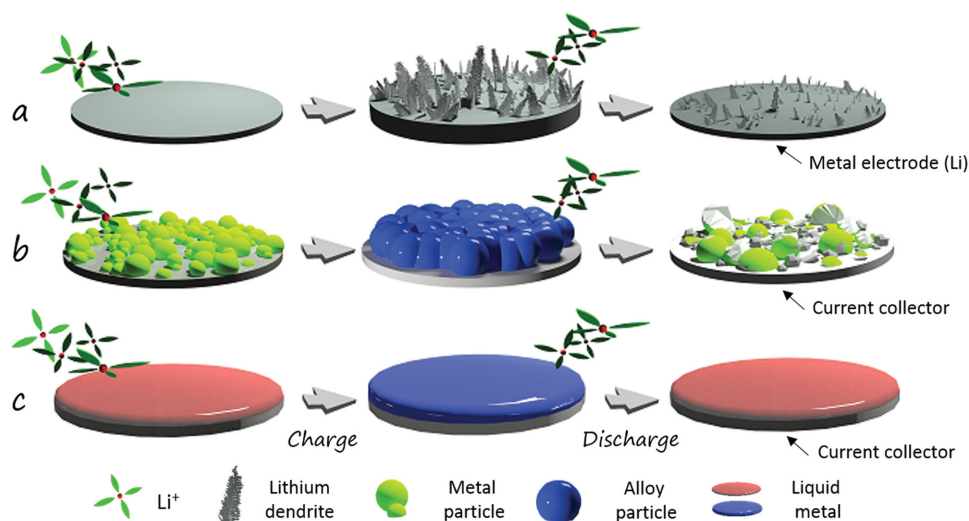


Figure 3. Schematics of: a) Na–S battery and the cross-section of the electrode and beta- Al<sub>2</sub>O<sub>3</sub> electrolyte, the arrow shows the Na<sup>+</sup> transportation direction during charge and discharge; Reproduced with permission.<sup>[2]</sup> Copyright 2011, The American Association for the Advancement of Science (AAAS), and b) ZEBRA battery with a secondary NaCl/AlCl<sub>3</sub> electrolyte. Reproduced with permission.<sup>[17]</sup> Copyright 2012, Elsevier.



**Figure 4.** Schematic illustrating the morphology/structure changing of solid (metal plate electrode (a)), metal/alloy composite electrode (b)) and liquid metal electrodes (c) during charging/discharging.

powder), and the salt is absorbed into the porous filler materials by capillary forces. The use of the paste electrolyte increases the safety of the cell by avoiding short circuits under conditions of movement. The paste electrolyte has been successfully applied in Li–Te,<sup>[27]</sup> Li–Bi<sup>[44]</sup> and Li–Se<sup>[45]</sup> cells, albeit with a high IR voltage loss from the low conductivity of paste electrolyte.

Lithium-tellurium cells with relatively high energy density were initially developed for electric vehicles applications, and much work at Argonne National Laboratory was undertaken to improve the specific energy and safety of the battery. The Li–Te liquid metal battery exhibited good cell performance, which could be possibly used in some specific fields, such as military applications. As for large-scale energy storage, in spite of the higher OCV, the high cost and low crustal abundance of Te hinders the deployment of Li–Te cell chemistry.

## 2.2. Li – Bismuth (Bi)

Bi is a semi-metal and of relatively low melting point (271.3 °C) and high electronegativity, which make it a good candidate for positive electrodes in LMBs. From the EMF measurements reported by Weppner and Huggins,<sup>[22]</sup> the OCV of pure Bi ranges from 0.95 to 0.72 V (vs Li/Li<sup>+</sup>) as the Li concentration in Bi ranging from 0 to 75%. As the Li concentration exceeds 75%, all Bi turns to Li<sub>3</sub>Bi (1130 °C), resulting in a sharp voltage drop. (see **Figure 6a**). In 1967, Na–Bi cell consisting of a liquid

Na anode and a liquid Bi cathode was reported.<sup>[27]</sup> In 1969, Li–Bi cell with LiF–LiCl–LiI paste electrolyte was reported to be working at a temperature from 380 °C to 485 °C.<sup>[44]</sup> The Li–Bi cell had a nominal cell voltage of  $\approx 0.6$  V at a discharge current density of 2.2 A cm<sup>-2</sup> (Figure 6b), and a maximum power density of 0.57 W cm<sup>-2</sup>. In a fully discharged state, the Li concentration in Bi was 41%, which was much lower than 75% obtained from the EMF measurements. The low utilization of Bi is due to a high Li concentration polarization under such high current density.

As the concept of LMBs were newly developed recently, Li–Bi cell with pure molten salt electrolyte re-attracted people's attention. A self-healing Li | LiCl–LiF | Bi cell working at 550 °C was reported by Ning, et al.<sup>[21]</sup> At 550 °C, the Li–Bi cell has good rate capability (> 70% capacity retention as the discharge current density ranged from 200 mA cm<sup>-2</sup> to 1250 mA cm<sup>-2</sup>, **Figure 7a**), and ultra-long cyclic performance (no obvious fading over 1000 cycles, **Figure 7b**). The battery was scaled up to 200 Ah capacity for a single cell (**Figure 7c** and **d**), which was a significant advance of LMBs for large-scale energy storage.

The post-mortem analysis showed that the Li concentration in Bi was close to 75at%, indicating that all Bi was turned into Li<sub>3</sub>Bi and agreed well with the EMF data.<sup>[22]</sup> According to the phase diagram of Li–Bi, a solid phase should be involved during discharge. However, during the charging process, the solid phase was turned back to pure liquid Bi, avoiding any dendrite formation and solid phase accumulation. More importantly, the

**Table 2.** Properties of typical liquid metal anodes and the anode-based batteries.

Anode	Melting point [°C]	Specific capacity [mAh g <sup>-1</sup> ]	Cost [\$ mol <sup>-1</sup> ]	Potential [vs. S.H.E.]	Solubility in molten salts [mol %]	Reported cells
Li	180	3862	0.43	-3.04	0.5–2.0 <sup>[18,19]</sup>	Li–Te, <sup>[20]</sup> Li–Bi, <sup>[21]</sup> Li–Sb, <sup>[22]</sup> Li–Sb–Pb <sup>[23]</sup>
Na	92.3	1165	0.057	-2.71	1.6–3.0 <sup>[18,24,25]</sup>	Na–Sn, <sup>[26]</sup> Na–Bi, <sup>[27]</sup> Na–S, <sup>[28]</sup> Zebra <sup>[29]</sup>
K	64	687.2	5.1	-2.93	4.9–19 <sup>[18,30]</sup>	K–Hg <sup>[31]</sup>
Ca	842	1340	0.14	-2.87	2.3–9.6 <sup>[18,32]</sup>	Ca–Bi, <sup>[33]</sup> Ca–Sb <sup>[34]</sup>
Mg	650	2233	0.069	-2.37	0.2–1.2 <sup>[18,35]</sup>	Mg–Sb <sup>[14]</sup>

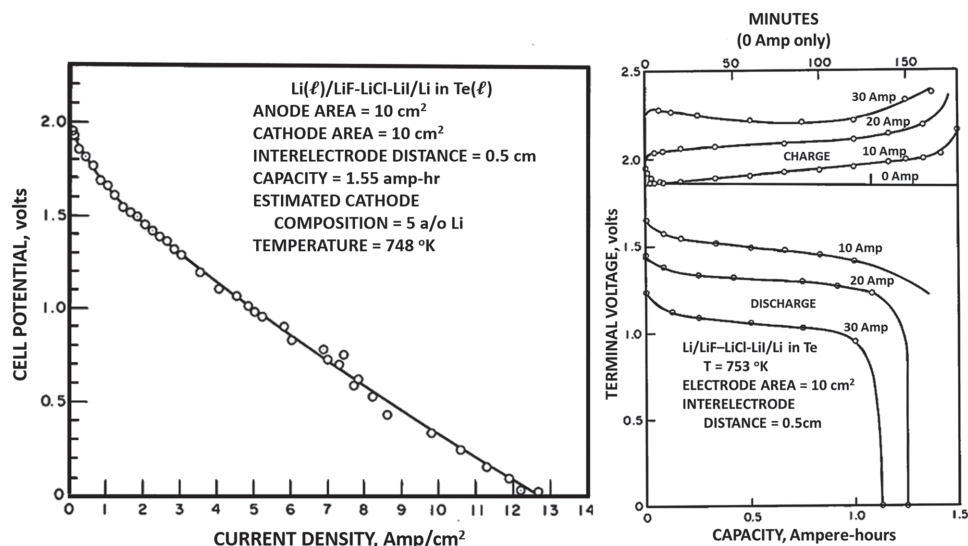


**Figure 5.** A Li|LiF–LiCl–LiI|Te bimetallic secondary cell developed at Argonne National Laboratory: the left is the cell voltage plot as a function of different current densities at 475 °C from a cell with 10 cm<sup>2</sup> electrodes area and 0.5 cm inter-electrode distance; the right are charge–discharge curves in a cell with 10 cm<sup>2</sup> electrodes area at 480 °C and the OCV curve as a comparison. Reproduced with permission.<sup>[20]</sup> Copyright 1967, Argonne National Laboratory.

formation of the solid phase did not cause high concentration polarization under 1000 mA cm<sup>-2</sup>, implying that the formed Li–Bi solid phase had high Li<sup>+</sup> conductivity and ensuring the high utilization of Bi.

Table 3 shows the properties of positive electrode candidates corresponding to Li negative electrode. Bi and Sb are both attractive for Li-based LMBs because of the relatively low cost and high OCV. However, despite the excellent performance, the high price (4.9 \$ mol<sup>-1</sup> and about 2.7 times to Sb) of Bi raises the cost of Li–Bi cell (> 220 \$ kWh<sup>-1</sup> for electrodes materials<sup>[21]</sup>) and thus prohibits its use for large-scale energy storage. In contrast, antimony (Sb) would be a good choice if it works at a much lower temperature than its melting point.

### 2.3. Li–Antimony (Sb) and Li–Lead (Pb) –Sb Cells

Sb is another semi-metal with high electronegativity that is also a good candidate for positive electrodes in LMBs. From the EMF measurements reported by Weppner and Huggins,<sup>[22]</sup> Sb has the similar thermodynamic properties to Bi. (see Figure 8) Due to the low-cost of Sb and high OCV of Li–Sb, Sb was considered as a promising positive electrode for LMBs. However, owing to its high melting point, a battery with a pure liquid Sb electrode should be operating at the temperature higher than 630 °C, which largely increases the costs of the secondary battery materials and corrosion issues. Therefore, reducing the operating temperature of batteries while maintaining the Sb-based electrodes at liquid

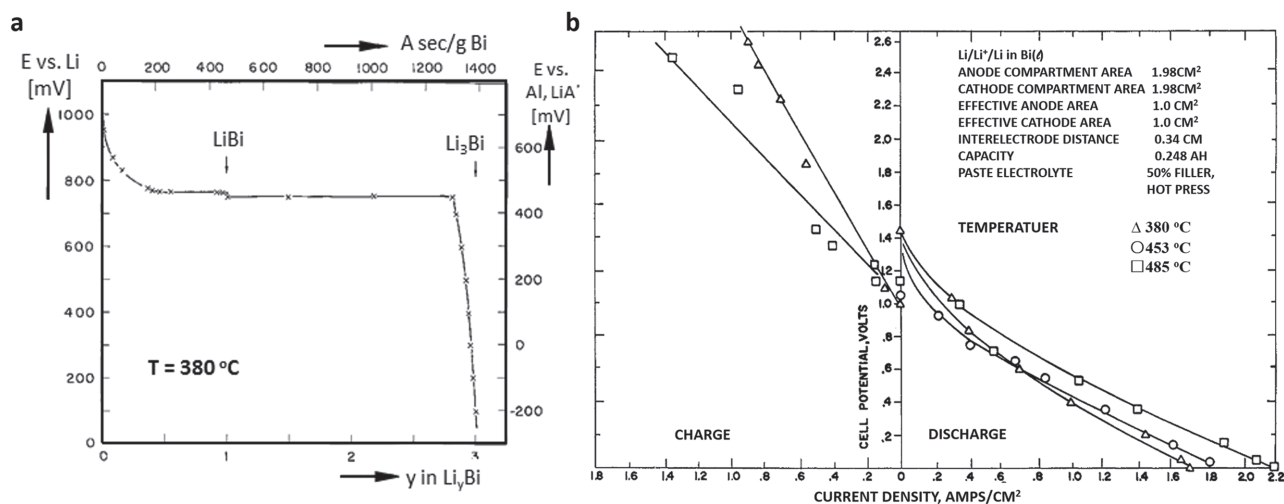


**Figure 6.** a) The coulometric titration curves from Li–Bi with LiF–LiCl–LiI molten salt electrolyte at 380 °C. The reference electrodes were Li–Al alloy in both of cells and the potential vs pure lithium were corrected for Li–Bi system. Reproduced with permission.<sup>[22]</sup> Copyright 1978, The Electrochemical Society (ECS). b) The steady-state voltage of the galvanic cell of Li–Bi with paste electrolytes as a function of charge–discharge current densities at 360 °C, 453 °C and 485 °C. Reproduced with permission.<sup>[44]</sup> Copyright 1969, Argonne National Laboratory.

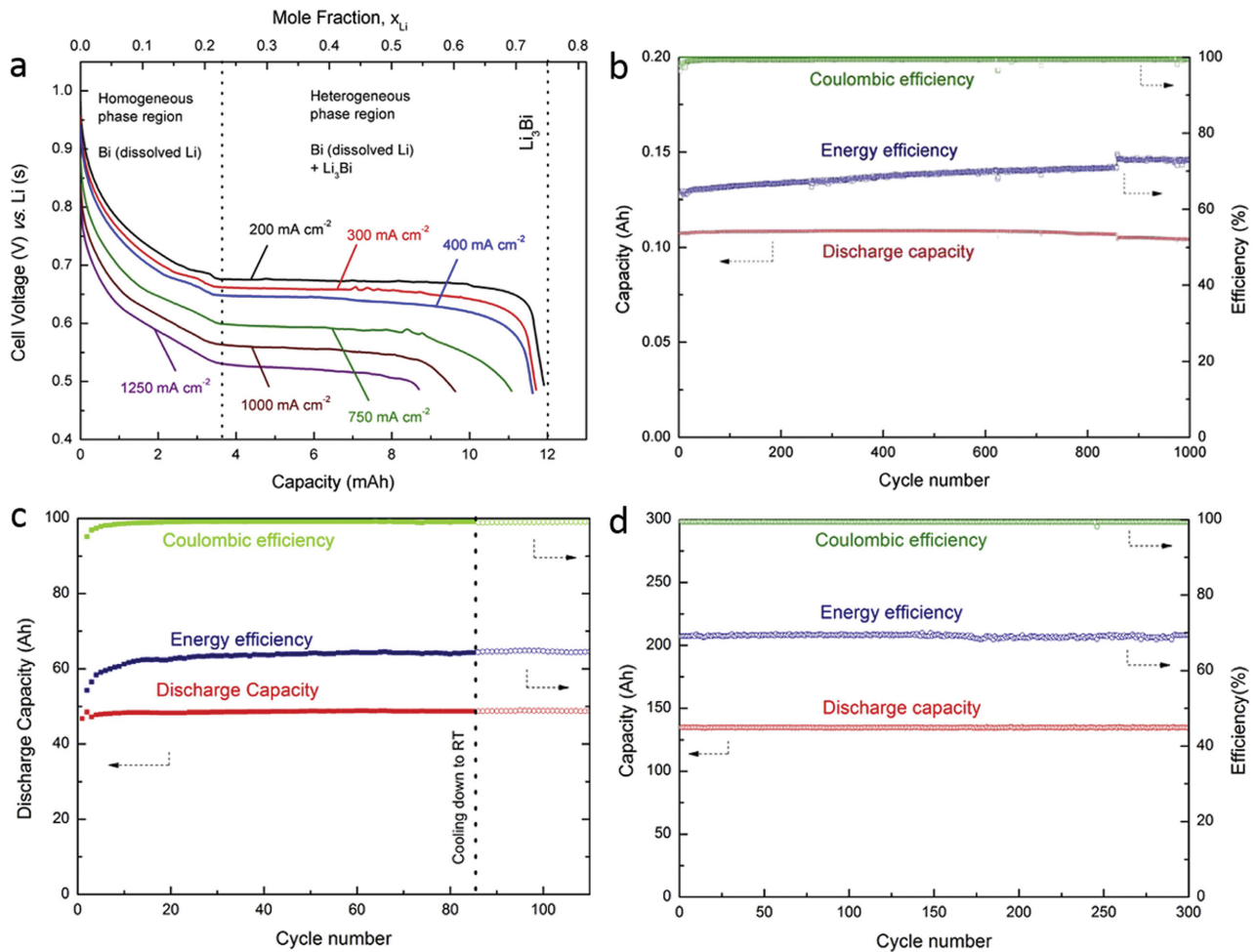


**Figure 7.** Electrochemical performance of LMBs of Li | LiF-LiCl | Bi: a) discharge curves at various current densities at temperature of 550 °C; b-d) are the cycling performance for different scale cells tested at  $0.3 \text{ A cm}^{-2}$ , b) is from 0.115 Ah theoretical capacity with 1.2 cm dia., c) 54.7 Ah and 10 cm dia., d) 143.25 Ah and 15 cm dia.. Reproduced with permission.<sup>[21]</sup> Copyright 2015, Elsevier.

state is an effective way to build high performance Sb-based LMBs. In 2014, Wang et al.<sup>[23]</sup>, reported that the low melting Pb-Sb eutectic alloy was an excellent positive electrode for Li-Sb-Pb batteries and the cell had a high OCV of 0.9 V. Pb was selected as the alloying metal due to its low cost ( $0.59 \text{ \$ mol}^{-1}$ ) and low melting point. In addition, there is no intermetallic

compound between Sb and Pb, and the electronegativity of Pb is smaller than Sb, meaning Pb acts only as a supporting element to decrease the melting point of Sb. Based on this invention, the operating temperature of LMBs was decreased to 450 °C, and the temperature could be further lowered to below 400 °C if the electrolyte compositions were optimized.

**Table 3.** Properties of typical liquid metal electrodes used for positive electrode in Li based LMBs.

Cathode candidate	Melting point [°C]	Density [ $\text{g cm}^{-3}$ ]	Cost [ $\text{\$ mol}^{-1}$ ]	OCV [vs. Li/Li <sup>+</sup> ]	Average OCV <sup>a)</sup>	Alloy stoichiometry	Capacity [Ah]	Reported chemistry
Te	449.5	6.24	44	≈1.7 V	> 1.5 V	Li <sub>2</sub> Te	1.55, 9.55	Li-Te <sup>[20,27,44]</sup>
Bi	271.3	10.05	4.9	≈0.95 V	< 0.8 V	Li <sub>3</sub> Bi	0.11, 48.8, 134	Li-Bi <sup>[21,44]</sup> Na-Bi <sup>[27]</sup>
Sb	630.7	6.70	1.8	≈0.92 V	≈0.9 V	Li <sub>3</sub> Sb	–	Li-Sb <sup>[22]</sup> Ca-Sb <sup>[46]</sup>
Sn	231.9	5.75–7.28	3.2	≈0.80 V	≈0.42 V	Li <sub>22</sub> Sn <sub>5</sub>	–	Li-Sn <sup>[47]</sup> Na-Sn <sup>[26]</sup>
Pb	327.5	11.34	0.52	≈0.75 V	≈0.50 V	Li <sub>7</sub> Pb <sub>2</sub>	–	Li-Pb <sup>[48]</sup>

<sup>a)</sup>Average OCV is the average value of OCV in a range from 0%mol Li in cathode metals to the final stoichiometry (vs Li/Li<sup>+</sup>).

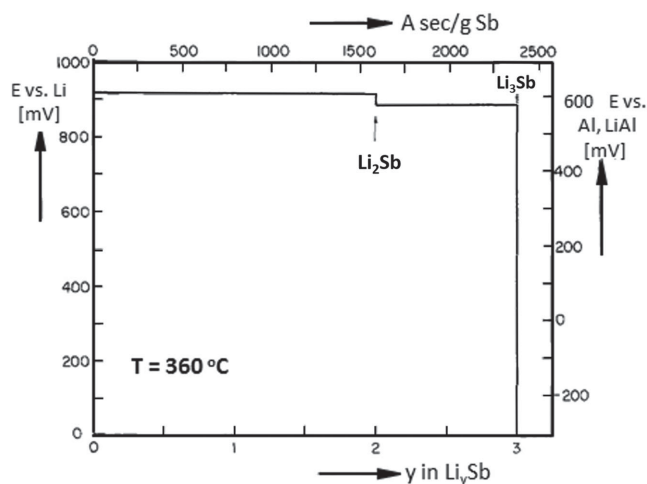


**Figure 8.** The coulometric titration curves from Li–Sb with LiF–LiCl–LiI molten salt electrolyte at 360 °C. The reference electrodes are Li–Al alloy in both cells and the potential vs pure lithium was corrected for the Li–Sb system. Reproduced with permission.<sup>[22]</sup> Copyright 1978, The Electrochemical Society (ECS).

A three-electrode cell with ternary molten salt electrolyte (LiF–LiCl–LiI) at 450 °C was designed to measure the EMF of Sb–Pb alloys and analyze the utilization of Sb in Sb–Pb alloys. The working electrodes are Sb–Pb alloys with different Sb/Pb ratios. As shown in **Figure 9a** and **b**, even the Sb–Pb alloy of low Sb concentration, e.g.,  $\text{Sb}_{18}\text{Pb}_{82}$ , still delivers high OCV of 0.87 V vs Li, which is only  $\approx 0.05$  V lower than the Li–Sb. In comparison with the Li–Pb, Sb–Pb alloy delivers much higher OCV than pure Pb (0.6 V), which indicates Sb is the only electrochemical active element in the electrode materials at a potential higher than 0.6V, and Pb is only the supporting component.

Excellent cell performance of Li | LiF–LiCl–LiI | Sb–Pb cells was reported by Wang, et al. Under a discharge current density of  $275 \text{ mA cm}^{-2}$ , the cells were of 0.7 V nominal discharge voltage, over 98% of Coulombic efficiency, with 73% of round-trip energy efficiency (Figure 9c and d). The cells had a good rate capability under charge–discharge current density from 100 to  $1000 \text{ mA cm}^{-2}$ , and the capacity retention was more than 50% of theoretical capacity at  $1000 \text{ mA cm}^{-2}$  (see Figure 9c). Moreover, the cells exhibited excellent cyclic performance that with 94% of the initial capacity maintained after 450 cycles (Figure 9b). Notably, the Li–Sb–Pb system also showed the ease of scalability from 1–2 Ah to 62 Ah for single cell in this work.

The use of Sb–Pb not only lowers the operating temperature and maintains the high OCV, more importantly, the introduction of Pb also reduces the cost of cells, which is key to its application in grid energy storage. As reported, the cost of the electrode materials for Li–Sb–Pb chemistry is less than  $69 \text{ \$ kWh}^{-1}$ , which is much lower than all of the aforementioned electrochemical cell systems and could potentially meet the metrics for large-scale energy storage. Moreover, the ultra-long cycle life and excellent efficiencies of the LMB enable it to be a competitive technology for energy storage. At Ambri, a 20 kWh LMB core has been tested, showing the application of this technology is getting closer to the market.<sup>[49]</sup>

Note that the discovery of using Sb–Pb alloy to lower the operating temperature of LMBs opens a new avenue to select proper electrodes and reduce the battery cost, which could also be broadly extended to other alloy chemistries for LMBs. Besides the binary alloys, ternary and multi-components alloys could be used for LMBs.

### 3. Sodium-Based Liquid Electrode

Besides the liquid Li electrode, liquid Na electrode is very attractive because of its low cost, earth-abundance, and environmental benignity. Although lithium-based batteries are currently dominating the energy storage market, their application in large-scale energy storage market is held back for their high cost and the uneven geological distribution of lithium sources, not to mention their fast capacity fade. Na-based batteries, such as Na–S and ZEBRA, have been demonstrated to be a promising choice for energy storage, and the research on Na-ion batteries is booming.<sup>[17,50–52]</sup> Sodium-based batteries are regarded by some as more suitable for large-scale energy storage. In this part, studies of liquid Na electrode based batteries will be reviewed.

#### 3.1. Sodium-Based LMBs

In 1960s, liquid sodium electrodes were used in bimetallic cells.<sup>[26,53–55]</sup> For example, Na–Sn<sup>[55,56]</sup> was initially adopted by General Motors for thermally regenerative bimetallic cells. The cell consisted of a liquid Na anode and Sn cathode, incorporating with NaCl–NaI electrolyte (Na | NaCl–NaI | Sn), which worked at 700 °C with cell voltage ranging from 0.33 to 0.43 V at  $0.7 \text{ A cm}^{-2}$ . The next cells with liquid sodium anode were studied by Argonne National Laboratory.<sup>[20,27]</sup> For example, the Na–Bi<sup>[20]</sup> cell with NaF–NaCl–NaI (15:32:53 mol%) electrolyte had been tested. A Na–Bi cell of 15 Ah theoretical capacity was assembled and operated at 580 °C. As shown in **Figure 10**, less than 80% of Coulombic efficiency was achieved when tested at  $665 \text{ mA cm}^{-2}$ , indicating that the cell has a high self-discharge rate. Moreover, the OCV dropped about  $\approx 0.12$  V after resting for 30 minutes, obviously implying self-discharge. It was found that the high self-discharge rates resulted from high solubility of sodium in molten salt electrolyte. Recently, Na–Bi cell was revisited and the cells showed the same performance. Therefore, suppressing the solubility of Na in molten salt is key to enabling liquid sodium to serve as the anode for batteries of high efficiency.<sup>[57]</sup>

There are two common approaches to reducing the Na solubility in molten salt. One approach is to optimize the composition of molten salt, for instance, use of multi-cation molten salts can suppress the solubility of metals.<sup>[58–60]</sup> Another way to reduce the Na solubility is reducing the operating temperature of sodium-based LMBs. However, it is difficult to find the sodium halide molten salt with a melting temperature lower than 500 °C. Hence, a suitable electrolyte is crucial for the development of liquid sodium electrode based batteries; the search turned from liquid electrolytes to the solid-state electrolytes (beta-alumina and NASICON). By using a solid ionic

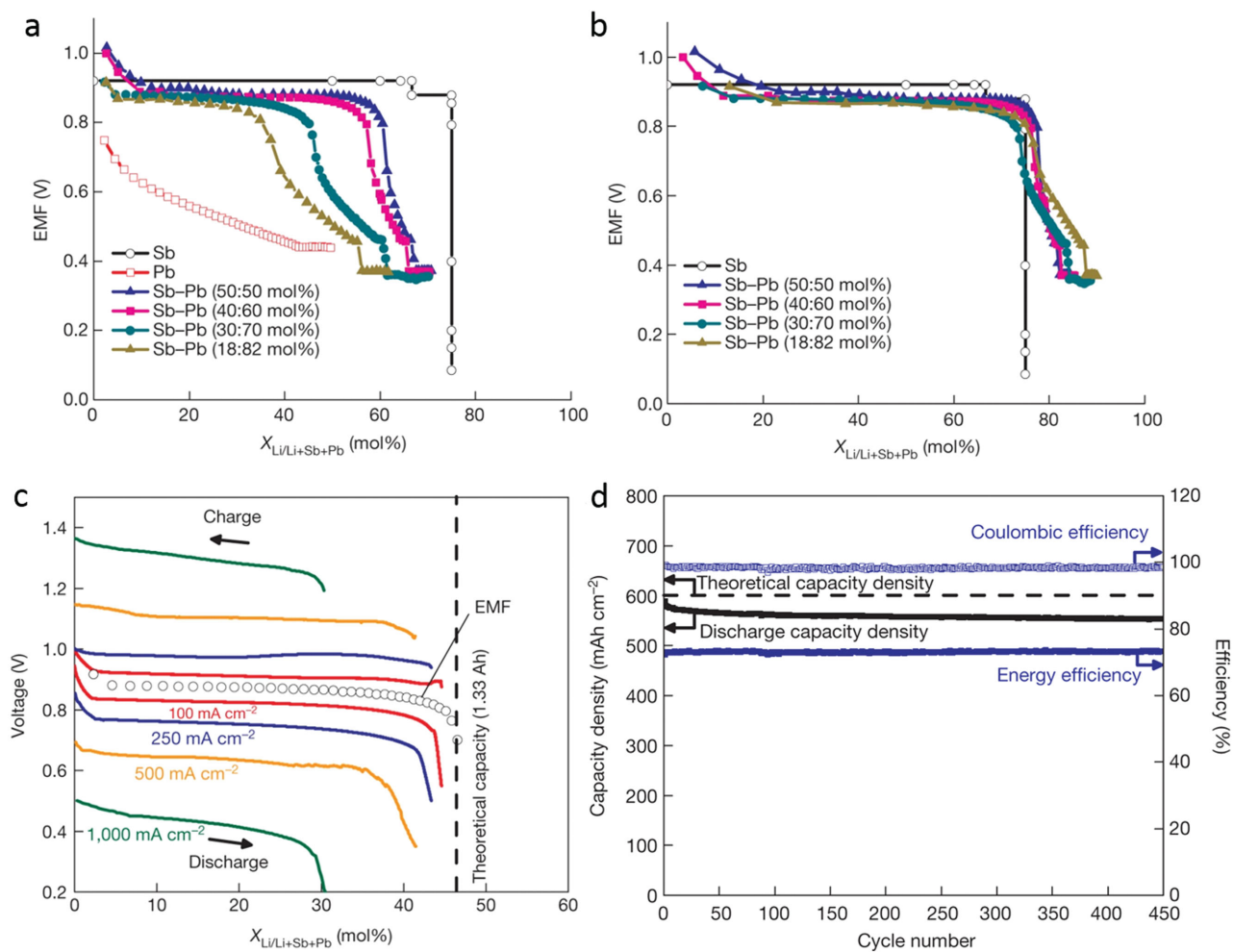


**Figure 9.** EMF of Li–Pb–Sb electrodes measured by coulometric titration in Li–Al|LiF–LiCl–Li|Li–Pb–Sb cells at 450 °C: a) EMF as a function of Li concentration in Sb–Pb alloys; b) as a function of Li concentration normalized with respect to Sb. The data of Li–Sb from the literature<sup>[22]</sup> is provided as a comparison. Electrochemical performance of Li | LiF–LiCl–Li | Pb–Sb cells: c) charge–discharge curves of a cell with 1.33 Ah theoretical capacity at current densities ranging from 100 mA cm<sup>-2</sup> to 1000 mA cm<sup>-2</sup>, and EMF curve as a comparison; d) capacity density, Coulombic efficiency and energy efficiency as function of cycle number, theoretical capacity of cell is 1.9 Ah. Reproduced with permission.<sup>[23]</sup> Copyright 2014, Nature Publishing Group.

selective membrane, the batteries can get rid of the molten salt electrolyte and the solubility of Na could be neglected. For example, Na–S and ZEBRA batteries with liquid Na electrode and beta-alumina solid electrolyte showed good cell performance and high Coulombic efficiency.

### 3.2. Sodium-Beta Al<sub>2</sub>O<sub>3</sub> Batteries

Na–S battery was pioneered at Ford in the United States in 1967,<sup>[28]</sup> and it has been primarily manufactured by NGK Insulators Ltd. in 2003. Sodium-metal halide batteries are referred to as ZEBRA (Zeolite Battery Research Africa Project) cells which are based on Na/NiCl<sub>2</sub> chemistry and were invented by Coetzer in 1978 and further developed by Beta Research and Development Ltd. in England until the technology was acquired by MES S.A.<sup>[29,61]</sup> Na–S and ZEBRA have similar designs using  $\beta/\beta''$ -Al<sub>2</sub>O<sub>3</sub> ceramic as a Na<sup>+</sup> conducting membrane.<sup>[62]</sup> The

beta-Al<sub>2</sub>O<sub>3</sub> allows only Na<sup>+</sup> transfer and is an insulator for electrons. To obtain the high ionic conductivity of solid-state electrolytes, Na–S and ZEBRA batteries operate at above 300 °C with liquid state Na anode. Both cells have gained tremendous attention for the potential energy storage applications due to their high energy density, high cell voltage, environmental friendliness, and nearly no self-discharge.<sup>[63]</sup> Despite these aforementioned merits, Na–S cells represents only the third ranking in installed capacity ( $\approx$ 3600 MWh) worldwide.<sup>[64]</sup> To reach more installed capacity of Na-beta alumina batteries, many challenges should be resolved in the practical application, such as: (1) high cost of large  $\beta''$ -Al<sub>2</sub>O<sub>3</sub> tube fabrication and cell seals; (2) low chemical stability of  $\beta''$ -Al<sub>2</sub>O<sub>3</sub> with some positive electrode materials like metal chloride in ZEBRA; (3) weak mechanical robustness to endure the vibrations.

The first strategy is to lower the operating temperature (below 200 °C) to decrease the solubility of positive electrode materials and the vapor pressure of Na, and thereby increase the stability of the  $\beta''$ -Al<sub>2</sub>O<sub>3</sub>. At a lower operating temperature, Na–S or

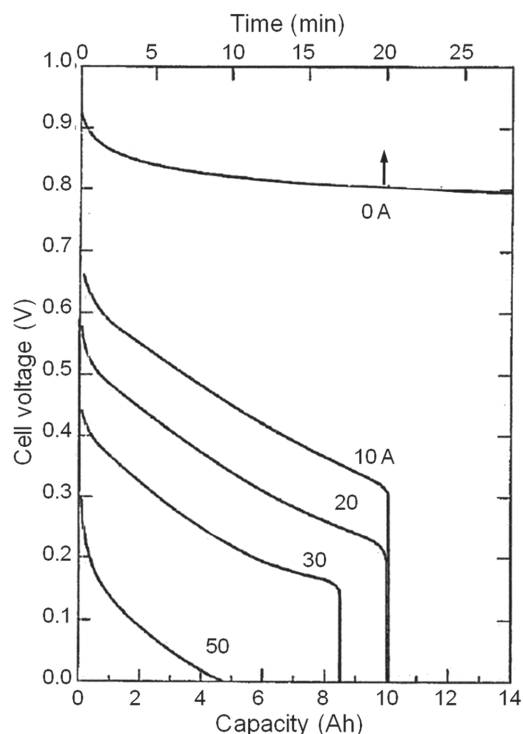


**Figure 10.** The discharge curves of Na | NaF–NaCl–NaI | Bi bimetallic secondary cell developed at Argonne National Laboratory, at various constant-current discharge rates, operated at temperature of 580 °C with 45 cm<sup>2</sup> electrode area and 0.4 cm distance between the two electrodes. Reproduced with permission.<sup>[20]</sup> Copyright 1967 Argonne National Laboratory.

ZEBRA battery enables the use of low-cost secondary battery materials, ease of sealing, lower maintenance fees.<sup>[65]</sup> Recently, another new low-temperature cell design was proposed by Lu et al.<sup>[66]</sup> at the Pacific Northwest National Laboratory. A ZEBRA battery with a planar composite ceramic electrolyte consisted of sintered  $\alpha$ -Al<sub>2</sub>O<sub>3</sub> and yttria-stabilized zirconia (YSZ) discs in loose  $\beta''$ -Al<sub>2</sub>O<sub>3</sub> powder was tested under 1/3 C rate at 175, 200, 240 and 280 °C, respectively. The results show that the battery is capable of being operated at a temperature below 200 °C

with better stability than that operated at temperature higher than 200 °C. Moreover, the operating temperature significantly affected the stability of cell as well as the cycling performance, for example, a higher operating temperature resulted in a more rapid cell polarization increase during cycling. As shown in **Figure 11**,  $\approx 55\%$  of cell resistance increase in end-of-charge polarization was observed at 280 °C after 60 cycles, while little resistance change was found in the cell cycled at 175 °C.

Notwithstanding the advantages of the low temperature operation, the disadvantages are bad wetting between the Na and  $\beta''$ -Al<sub>2</sub>O<sub>3</sub>, and lower Na<sup>+</sup> conductivity. To reduce the resistance at the interface between liquid Na electrode and  $\beta''$ -Al<sub>2</sub>O<sub>3</sub>, it is necessary to enhance wettability.<sup>[67]</sup> Approaches include pre-treatment in vacuum<sup>[68]</sup> or reaction with sodium<sup>[69]</sup> to remove absorbed surface moisture, and coating with carbon/PbO.<sup>[70]</sup> W.G. Bugden et al.<sup>[71]</sup> found that doping a certain amount of Li<sup>+</sup> and Na<sup>+</sup> in electrolyte could suppress the rise in cell resistance dramatically. David Reed et al.<sup>[72]</sup> reported that a thin Sn film on the surface of  $\beta''$ -Al<sub>2</sub>O<sub>3</sub> / YSZ can help Na wet the  $\beta''$ -Al<sub>2</sub>O<sub>3</sub>/YSZ surface better. One year later, Lu et al.<sup>[73]</sup> reported that an alloying strategy can remarkably improve the wetting at much lower temperature (< 100 °C). Cesium (Cs) was alloyed with sodium to remarkably improve the wetting between Na and  $\beta''$ -Al<sub>2</sub>O<sub>3</sub> because of the lower surface tension of liquid cesium, and stronger interactions between Cs and  $\beta''$ -Al<sub>2</sub>O<sub>3</sub> verified by computational and experimental studies. By using the same strategy, a Na–S cell with Na–Cs alloy anodes was cycled under 2.33 mA cm<sup>-2</sup> at 150 °C showing significant improvement in cycle life over pure sodium anodes (see **Figure 12**). More importantly, with the Na–Cs alloy anode, the Na(Cs)–S cell was able to be cycled under 1/7 C rate with a high capacity of 330 mAh g<sup>-1</sup> at a temperature below 100 °C and showed excellent stability with slight degradation in cell capacity (see **Figure 13**).

However, the lower operating temperature results in poorer ionic conductivity of the solid-state electrolyte and therefore increases IR drop. One direct way to decrease the resistance is to reduce the thickness of the solid membrane. Further efforts in terms of developing a better Na<sup>+</sup> conductive solid-state electrolyte at low operating temperature is under investigation.

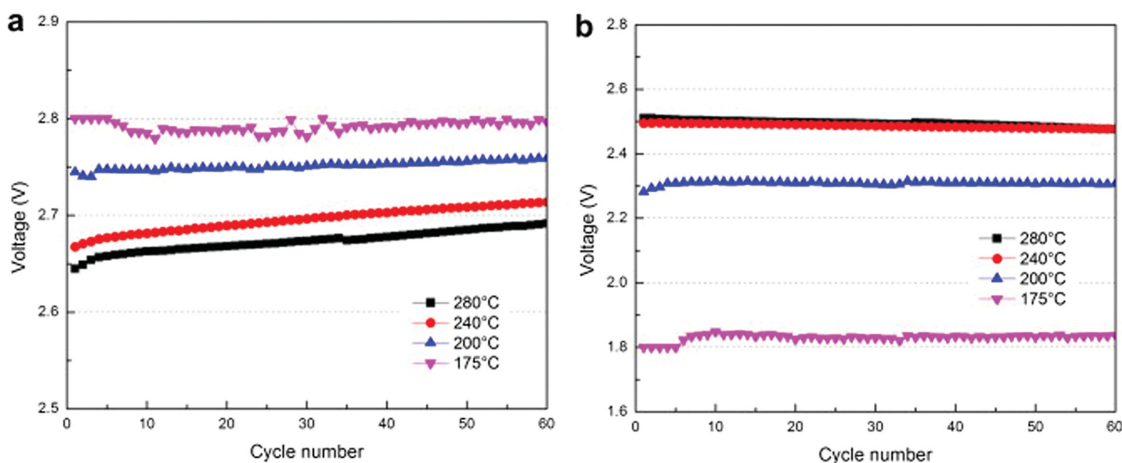


**Figure 11.** Cell voltage (a) and corresponding cell resistance (b) of the cells tested at various temperatures at the end of charging. Reproduced with permission.<sup>[66]</sup> Copyright 2012, Elsevier.

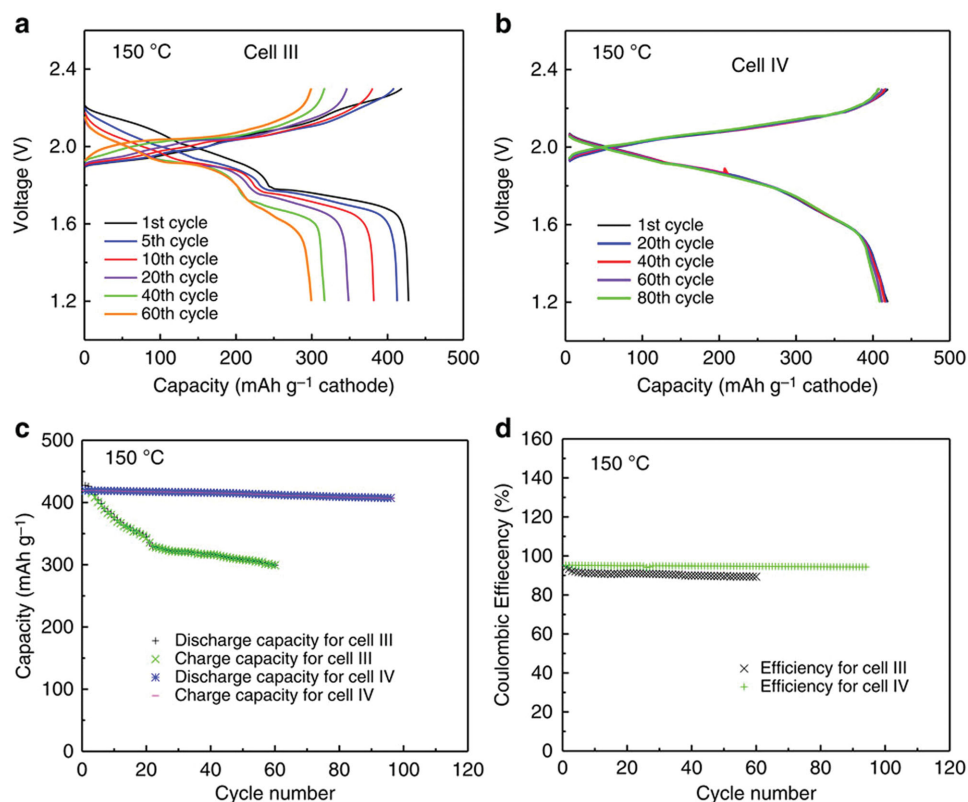


**Figure 12.** Cell III: Na|Pb-treated BASE|S with tetraglyme plus 1M NaI and cell IV: Na-Cs|untreated BASE|S with tetraglyme plus 1M NaI. Cell voltage profiles for cell III (a) and cell IV (b) at 150 °C. Comparison of discharge/charge capacity (c) and Coulombic efficiency (d) during cycling between cell III and cell IV. Reproduced with permission.<sup>[73]</sup> Copyright 2015, Nature Publishing Group.

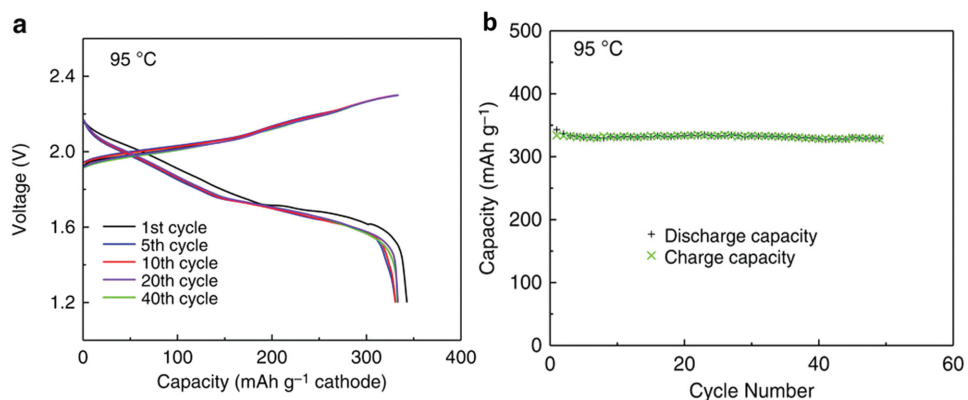
Besides the  $\beta''$ -Al<sub>2</sub>O<sub>3</sub>, other solid-state electrolytes, such as NASICON,<sup>[74]</sup> are being studied and showing good Na<sup>+</sup> conductivity under 200 °C. A battery employing the NASICON electrolyte will be discussed below.

Table 4 shows the comparison of Na-based LMBs and Na-beta alumina batteries, and the properties of other LMEs batteries including K-Hg, Mg-Sb and Ca-based systems. In the next part, we will mainly focus on the recent development of K, Mg and Ca-based systems.

## 4. Potassium, Magnesium and Calcium-Based Liquid Electrodes

### 4.1. Potassium

Potassium (K) has a low melting point of 64 °C and a very low electronegativity close to Li. Constrained by the operating temperature, liquid mercury (Hg) is an ideal positive electrode coupled with the liquid K electrode. In 1960, the thermally



**Figure 13.** Cell voltage profiles and discharge/charge capacities for cell of Na-Cs|untreated BASE|S with tetraglyme plus 1M NaI operating at 95 °C. Reproduced with permission.<sup>[73]</sup> Copyright 2015, Nature Publishing Group.

**Table 4.** Properties of typical electrodes used for liquid metal electrode batteries beyond Li-based system.

Anode	Cathode	OCV (V)	Average OCV (V)	Products	Capacity [Ah]	Ref.
Na	Bi	≈0.74	≈0.65	Na <sub>3</sub> Bi	15	[20,27,57]
	Sb	≈0.86	≈0.8	Na <sub>3</sub> Sb	–	[57]
	Sn	≈0.5	≈0.35	NaSn	–	[26,57]
	Pb	≈0.47	≈0.3	Na <sub>9</sub> Pb <sub>4</sub>	–	[57]
	S	2.08	≈1.9	Na <sub>2</sub> S <sub>2</sub>	~ 650	[12,28]
K	NiCl <sub>2</sub>	2.58	2.58	Ni (NaCl) <sub>2</sub>	< 650	[12,29]
	Hg	0.72	–	–	0.2	[57,31]
Mg	Sb	0.51	0.39	Mg <sub>12</sub> Sb <sub>88</sub>	4.0, 7.0	[14]
Ca	Bi	0.9	0.8	Ca <sub>5</sub> Bi <sub>3</sub>	–	[33,74]
	Sb	1.04	0.94	Ca <sub>2</sub> Sb	0.57, 1.08, 1.33	[34,46,80]

“recharged” battery was the earliest model of LMB proposed by General Motors.<sup>[31]</sup> K and Hg were respectively selected as negative and positive electrodes, and KOH–KBr–KI was the electrolyte, as shown in **Figure 14**. K–Hg cells were successfully cycled at a current density of 94 mA cm<sup>-2</sup> under 300 °C with a Coulombic efficiency of 90–95%. Moreover, the cell was cycled for 60h, and a power density of 48 mW cm<sup>-2</sup> was realized in a thermal regenerative system with a conjunction of three cells. However, due to the toxicity and high vapor pressure of Hg, it is impractical to use the K–Hg battery for large-scale energy storage.

#### 4.2. Mg–Sb

As an earth-abundant element with a melting temperature of 650 °C, magnesium is a promising liquid metal electrode for batteries. Unlike the Li, Na, and K, one Mg atom can release two electrons when it is oxidized, possessing a higher gravimetric capacity. Because of Mg has extremely low solubility in molten salt electrolytes, a battery with a liquid Mg electrode should have low self-discharge rate and high Coulombic efficiency. In 2012, Bradwell et al.<sup>[14]</sup> assembled an Mg–Sb cell with a liquid Mg anode, a liquid Sb cathode, and NaCl–KCl–MgCl<sub>2</sub> electrolyte; the cell exhibited good cell performance at 700 °C. Under 100 mA cm<sup>-2</sup>, the nominal discharge cell voltage was about 0.35 V and the Coulombic and energy efficiencies are 94% and 73%, respectively. (**Figure 15**) In a fully discharged state, the composition of the positive electrode was estimated as Mg<sub>12</sub>Sb<sub>88</sub> which was transformed into two phases of Sb and Mg<sub>3</sub>Sb<sub>2</sub> after cooling to room temperature.

From the point of view of materials prices, the Mg–Sb cell may be a suitable

candidate chemistry for LMBs along with its excellent electrochemical performance. At the beginning, Mg–Sb cell is not attractive for practical application due to the high melting point of magnesium (648 °C) and antimony (630 °C) and low OCV of Mg–Sb. The cost of electrode materials calculated in

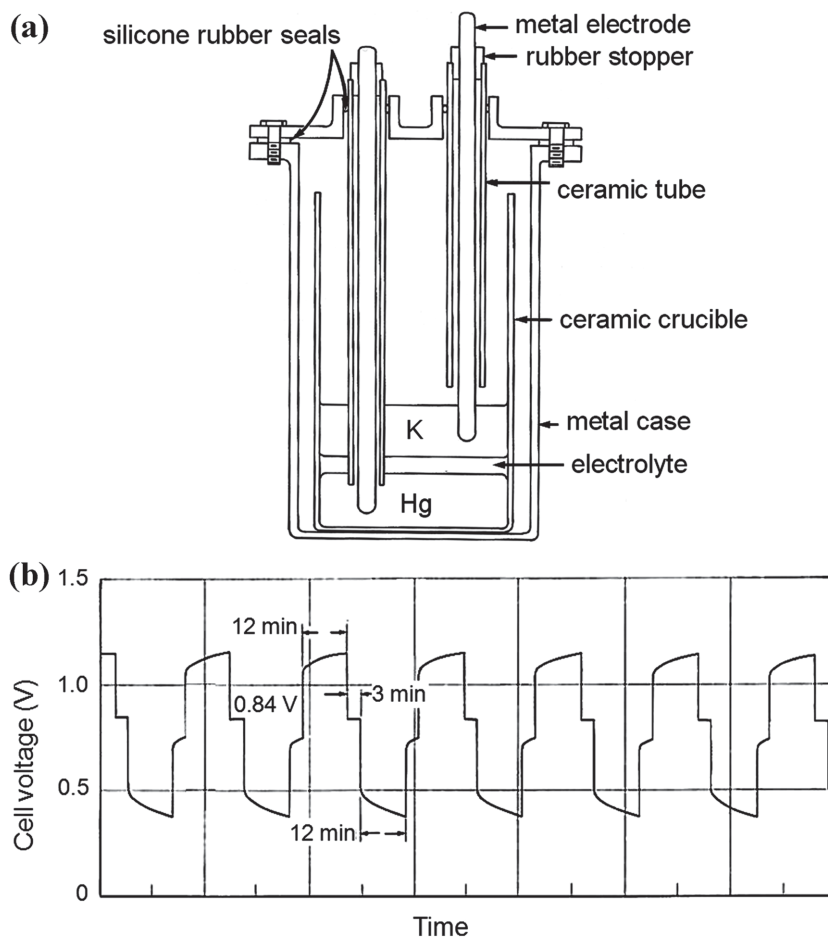


**Figure 14.** A K | KOH–KBr–KI | Hg liquid metal cell developed at General Motors Corporation. a) Schematic diagram and b) charge/discharge curves of the cell at 87 mA cm<sup>-2</sup> and 300 °C with an electrode area of 11.5 cm<sup>2</sup> and electrolyte thickness of 1.5 cm. Reproduced with permission.<sup>[31]</sup> Copyright 1967, American Chemical Society (ACS).

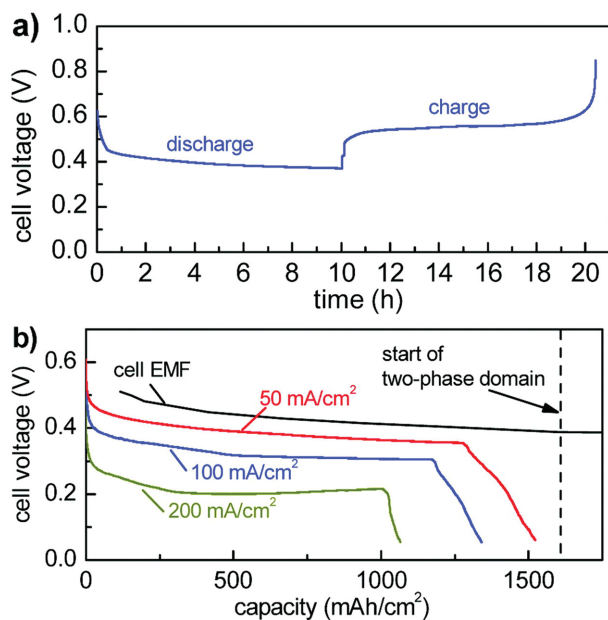


**Figure 15.** Electrochemical performance of an Mg|NaCl–KCl–MgCl<sub>2</sub>|Sb battery operated at 700 °C. a) A typical charge–discharge curve of cell with current density of 50 mA cm<sup>-2</sup>. b) EMF profile and rate capability test with various current densities. Reproduced with permission.<sup>[14]</sup> Copyright 2012, American Chemical Society (ACS).

this work was 170 \$ kWh<sup>-1</sup>. Due to high operating temperature, the low cell voltage and limited rate capability, Mg–Sb cells are far away from the real application in large-scale energy storage.

### 4.3. Calcium-Based Systems

Calcium is another earth-abundant element with a low electronegativity, but its melting point is too high (842 °C) to be directly used for LMBs. Due to its low cost and electronegativity, calcium was initially used as negative electrode in thermal batteries from 1950 to 1980.<sup>[39,75]</sup> Due to its low cost (0.14 \$ mol<sup>-1</sup>) and earth-abundance calcium attracted much attention after the concept of LMBs had been proposed. However, the use of calcium for LMBs faces two challenges: high melting point of calcium (842 °C) and high solubility of calcium in molten salt electrolytes.

The EMF of Ca-based electrodes were measured in a three-electrode setup.<sup>[46,76]</sup> To reduce the effect of soluble Ca in molten salts, solid-state CaF<sub>2</sub> (melting point 1402 °C) of acceptable Ca<sup>2+</sup> conductivity was used as solid electrolyte to measure EMF data. For example, a Ca(s) | CaF<sub>2</sub>(s) | Ca (in Bi) three-electrode cell was designed to investigate the thermodynamic properties of calcium-bismuth alloy.<sup>[33,76]</sup> As shown in **Figure 16a**, the average OCV of Ca–Bi was ≈0.8V at a temperature range of 600–800 °C. Only a high-melting-point phase of Ca<sub>5</sub>Sb<sub>3</sub> (1653 °C) formed and then resulted in the obvious voltage drop during the process of calcification (Figure 16b). Poizeau et al.<sup>[46]</sup> used the same cell design of solid-state electrolyte to investigate Ca–Sb system, and a cell (Ca(s) | CaF<sub>2</sub> | Ca–Sb) was assembled at temperature of 550–830 °C. The average OCV of Ca–Sb of

was ca. 1.0 V, which was 0.2V higher than that of Ca–Bi, as shown in **Figure 16c**. In addition, Poizeau first attempted to explain the interaction of liquid metal particles by both regular associated solution model<sup>[77]</sup> and the molecular interaction volume model (MIVM).<sup>[78]</sup>

According to the EMF data, Ca-based LMEs have a relatively high OCV, indicating that Ca is a good candidate LME for LMBs. To realize the Ca-based LMBs, one important strategy is to lower the melting temperature of Ca-based electrodes. Like the strategy used for Sb–Pb electrode, alloying is an effective way to bring down the operating temperature. Newhouse et al.<sup>[79]</sup> reported that alloying Mg with Ca to form low-melting Ca–Mg alloy (eutectic temperature of Ca–Mg is 440 °C). As the electronegativity of Ca is much lower than that of Mg, Ca behaves as active electrode materials in Ca–Mg eutectic. Accordingly, a Ca (in Bi) | CaF<sub>2</sub> | Ca (in Mg) cell revealed that a Ca–Mg alloy of high Ca concentration (0.60 < x<sub>Ca</sub> < 0.80) would only decrease the cell voltage by less than 30 mV compared with the pure Ca. And a cell of a Ca–Mg alloy with low Ca concentration (0.05 < x<sub>Ca</sub> < 0.15) had a voltage of ≈200 mV less than that of the cell with pure Ca anode. Moreover, the Ca–Mg alloy of low Ca concentration decreased the solubility of Ca in the molten salt by almost two orders of magnitude (see **Figure 16d**). More recently, Ouchi et al.<sup>[80]</sup> reported a Ca–Mg | LiCl–CaCl<sub>2</sub> | Bi cell, operating at 550 °C, achieving 99% of Coulombic efficiency and excellent cycling performance, which further confirmed the above results.

In 2013, a three-electrode cell of Ca–Bi | LiCl–NaCl–CaCl<sub>2</sub> | Bi was reported by Kim et al.<sup>[33]</sup> The cell with molten salt electrolytes (LiCl–NaCl–CaCl<sub>2</sub> 38–27–35mol%, T<sub>m</sub> = 450 °C) showed similar results of the cell with solid CaF<sub>2</sub> electrolyte by coulometric titration, as shown in **Figure 17a**, agreeing well with the results of the cell using solid CaF<sub>2</sub> electrolyte. From the results of self-discharge study (Figure 17b), the dissolution of calcium in molten salt electrolytes can be suppressed through alloying with Bi. More recently, the Ca–Sb LMBs with LiCl–NaCl–CaCl<sub>2</sub> electrolyte was investigated by Ouchi,<sup>[34]</sup> and a Coulombic efficiency of almost 100% was obtained. Consequently it is confirmed that the dissolution of Ca from Ca–Mg into molten salt electrolytes is suppressed by alloying and the use of multi-cation electrolyte. Compared with the Ca–Bi cell, Ca–Sb cells had a higher discharge cell voltage (≈0.1 V higher) (**Figure 18**), better cycle performance, smaller capacity fade (< 0.01% cyc<sup>-1</sup>), and low capital cost of the electrode and electrolyte materials (< 90 \$ kWh<sup>-1</sup>).

Overall, the eutectic Ca–Mg alloys enabled the liquid Ca-based electrodes to work at lower temperature, suppressing the solubility of Ca in Ca-based molten salt electrolytes and achieving good cell performance. However, more efforts are needed to further decrease the operating temperature and bring down the cost of the battery.

## 5. Electrolyte and Other Key Issues

The electrolyte is an indispensable part in both LMBs and Na-beta alumina batteries. With the use of liquid metal electrodes in batteries, molten salt electrolyte, solid-state β"-Al<sub>2</sub>O<sub>3</sub>, NASICON and glass electrolytes were employed

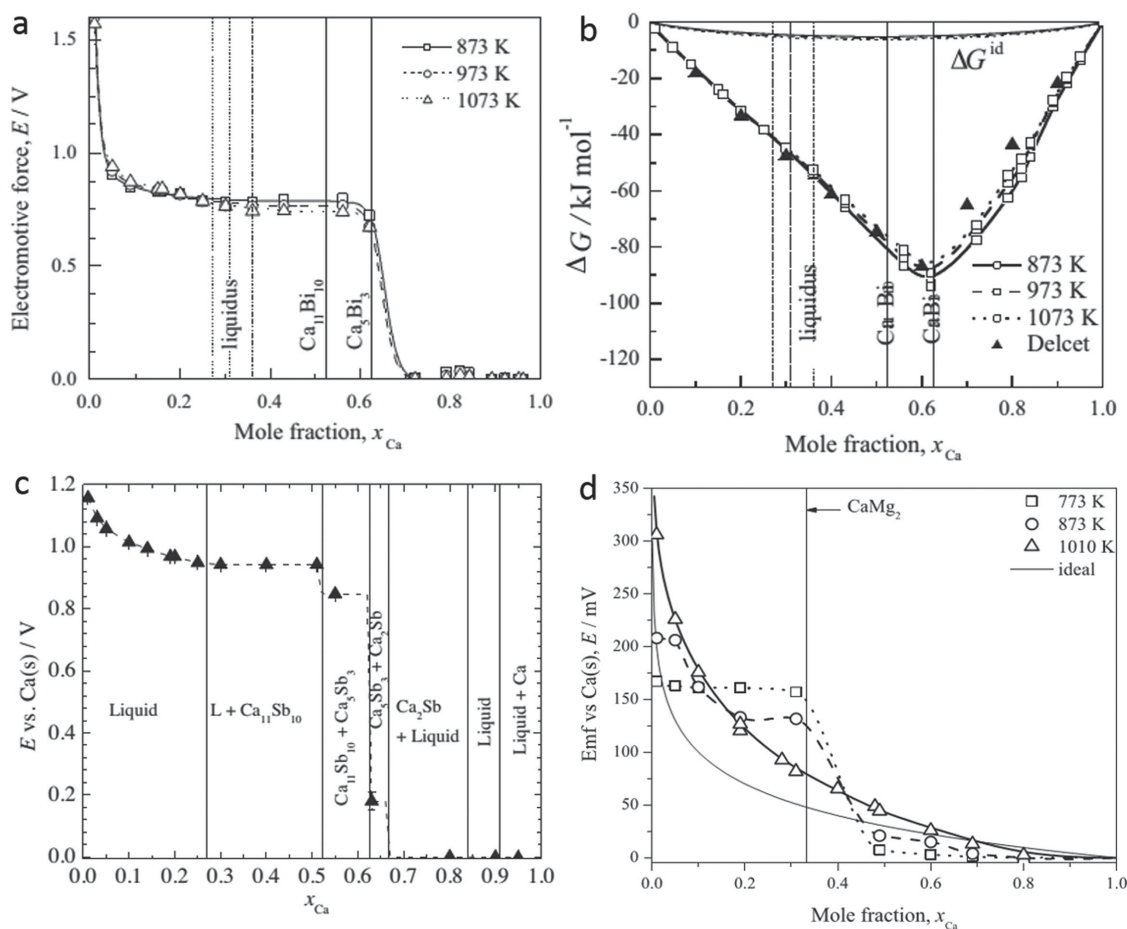


**Figure 16.** EMF and thermodynamic data obtained by coulometric titration. a) EMF measurements from a Ca(s) | CaF<sub>2</sub>(s) | Ca(in Bi) cell at different temperatures and b) Gibbs free energy  $\Delta G$  and  $\Delta G^{\text{id}}$  as a function of calcium mole fraction in bismuth  $x_{\text{Ca}}$ . Reproduced with permission.<sup>[76]</sup> Copyright 2012, Elsevier; c) EMF measurements of Ca(s) | CaF<sub>2</sub> | Ca–Sb cells at 700 °C. Reproduced with permission.<sup>[46]</sup> Copyright 2012, Elsevier; d) EMF measurements of Ca (in Bi) | CaF<sub>2</sub> | Ca(in Mg) cells and the expected EMF curves for an ideal solution at 737 °C. Reproduced with permission.<sup>[79]</sup> Copyright 2013, Elsevier.

depending on the compatibility of electrodes with the electrolytes. Besides electrolytes, hermetic cells are crucial for protecting the liquid metal electrodes, and the seals of the cells should be considered since some liquid metal electrodes are

highly reactive and have high vapor pressure. In addition, the corrosion in the cell is highly related to the lifetime of cell, which is important for selecting secondary battery materials at elevated temperature.

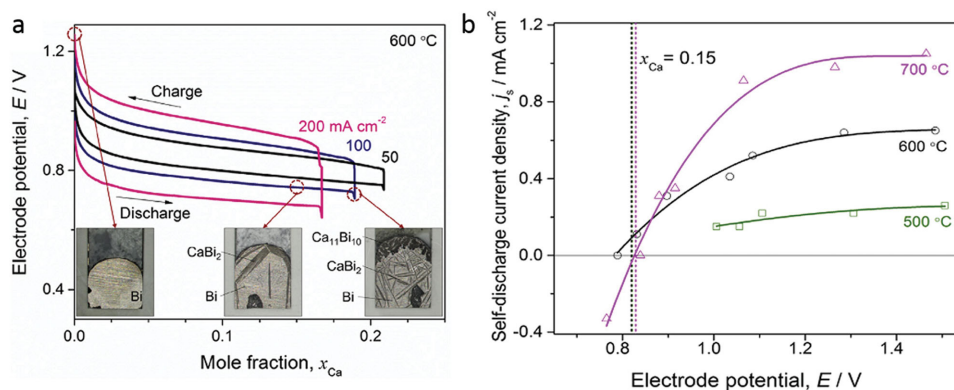


**Figure 17.** Cell performance and self-discharge investigation of Ca–Bi | LiCl–NaCl–CaCl<sub>2</sub> | Bi cells: a) charge/discharge curves of Ca–Bi | LiCl–NaCl–CaCl<sub>2</sub> | Bi cells at different current densities and post-mortem analysis, b) self-discharge current densities of electrodes of  $x_{\text{Ca}} = 0.15$ , measured at 500 °C, 600 °C, 700 °C in above cells. Reproduced with permission.<sup>[33]</sup> Copyright 2015, Elsevier.

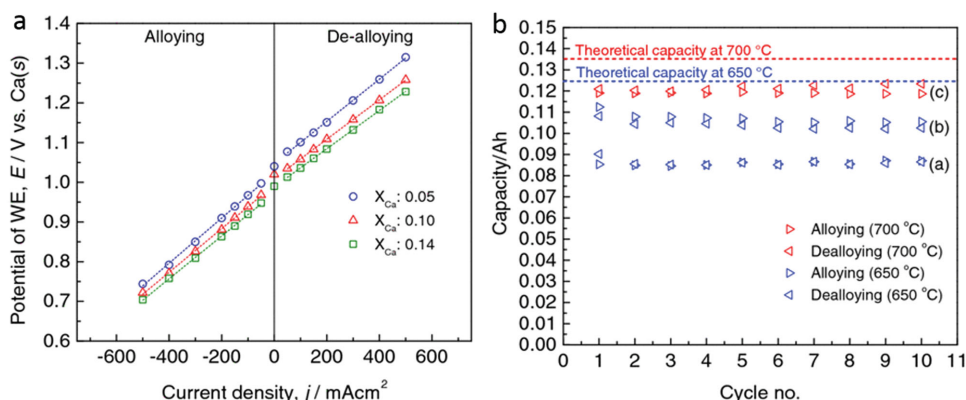


**Figure 18.** a) The potential of WE ( $SbCa_x$ ) and the  $E_{eq}$  as a function of current density at 650 °C  $x_{Ca}$  (in Sb) = 0.05, 0.1 and 0.14. b) The capacities of the alloying and dealloying processes with the progression of cycles. Current densities were (a, c) 200 mA cm<sup>-2</sup> and (b) 50 mA cm<sup>-2</sup>. Reproduced with permission.<sup>[34]</sup> Copyright 2014, The Electrochemical Society (ECS).

### 5.1. Molten Salt Electrolytes for LMB

The molten salt electrolyte layer in LMBs is a strong ionic conductor and an electron insulator to block electron transport between the two liquid metal layers. The liquid metals/alloys at both electrodes are designed to be insoluble in molten salts, obviating the need for an extra ionic selective membrane. Clearly, the compatibility of molten salt with the liquid metal and/or alloys is paramount to the cell performance of LMBs. The selection of molten salt electrolyte for liquid metal electrodes should comply with the following criteria: (1) low melting point; (2) high ionic conductivity; (3) appropriate density; (4) no spontaneous reactions between the electrodes and electrolyte; (5) immiscibility with the liquid metal/ alloy electrodes. Among these requirements, the solubility of liquid metal/alloys in molten salt electrolyte is the main challenge in LMBs, e.g., Na and Ca can dissolve in the molten salt to some degree, conducting electrons through the electrolyte and thereby resulting in self-discharge and low round-trip efficiencies. The solubility of metal in molten salts was discussed by Kim et al.<sup>[57]</sup> It was reported that the use of multi-cation molten salt will reduce the solubility of the metal and lower the melting temperature of the molten salt as well.

Due to the highly ionic conductivity, small IR drop corresponds to high voltage efficiency at high charge/discharge rate. Generally, the mobility of ions in molten salts follows Arrhenius-type behavior, therefore, the higher mobility of ions the better ionic conductivity of molten salt. P. Masset et al.<sup>[40]</sup> have summarized the experimental investigations of conductivity measurements of high-temperature molten salts and pointed out that lithium-based molten salts present the highest ionic conductivities based on the higher mobility of lithium cation than other alkali-metal cations, especially in iodide-based molten salts. As shown in Table 5, conductivity and other properties of several kinds of alkali and alkaline-earth halides commonly used in LMB are summarized. As can be seen, LiI-based molten salt electrolytes can supply over 3.5 S cm<sup>-1</sup> of conductivity which is one of the highest values in molten salts.

### 5.2. Beta-Al<sub>2</sub>O<sub>3</sub>, NASICON and Glass–Ceramic

Because liquid metals have high solubility in molten salt electrolyte, solid-state electrolytes could solve this problem, for instance, Na–S and ZEBRA batteries with a solid ceramic electrolyte ( $\beta$ -Al<sub>2</sub>O<sub>3</sub>) achieve high Coulombic efficiencies. The use of  $\beta$ -Al<sub>2</sub>O<sub>3</sub> completely avoids direct contact of the anode and cathode, and thereby minimizing the self-discharge of the battery. Similar to the molten salt electrolyte, a solid-state electrolyte should meet the following requirements: (1) high enough ionic conductivity and selectivity; (2) thermodynamically and mechanically stable over a wide temperature range; (3) physicochemically compatible with anode, cathode and secondary electrolyte.

Among all the aforementioned LMEs, Na has low melting point and milder reductive ability compared with Li and Ca. The Na<sup>+</sup> selective membrane has attracted much attention for a long time. Since the invention of  $\beta/\beta'$ -Al<sub>2</sub>O<sub>3</sub>, Na–S and ZEBRA batteries have developed rapidly. Many methods were studied to synthesize  $\beta'$ -Al<sub>2</sub>O<sub>3</sub> aiming to improve its ionic conductivity and mechanical strength, such as solid-state reaction,<sup>[92]</sup> sol-gel process,<sup>[93,94]</sup> co-precipitation technique,<sup>[95]</sup> spray-freeze/freeze-drying<sup>[96]</sup> and microwave heating methods.<sup>[97]</sup> The ionic conductivity of  $\beta/\beta'$ -Al<sub>2</sub>O<sub>3</sub> at different temperatures is presented in Figure 19. To enhance the strength and the fracture toughness, the  $\beta'$ -Al<sub>2</sub>O<sub>3</sub> was doped with ZrO<sub>2</sub>. Unfortunately, this caused a decrease in ionic conductivity. Many other approaches were studied to modify  $\beta'$ -Al<sub>2</sub>O<sub>3</sub> by doping with Li<sup>+</sup> and Mg<sup>2+</sup> to improve the Na<sup>+</sup> conductivity.<sup>[66]</sup> In addition to the conductivity, frangibility of the  $\beta/\beta'$ -Al<sub>2</sub>O<sub>3</sub> is a vital safety concern because it will cause cell failure and even fire when the liquid Na anode contacts the cathode at elevated temperatures. So the production of the ceramic separator is stringent and needs complicated processes to cautiously control the microstructure of the  $\beta/\beta'$ -Al<sub>2</sub>O<sub>3</sub> and then ensure the robustness of the ceramics. Although large-scale production of this ceramic has been achieved, the low production yields and high cost are still the major concerns.

In addition to  $\beta/\beta'$ -Al<sub>2</sub>O<sub>3</sub>, NASICON-type, glass and glass–ceramic have been developed for sodium-based batteries with

**Table 5.** Properties of common molten halide salts electrolyte systems.

Electrolyte	Composition [mol%]	Melting point [°C]	Density		Ionic conductivity At 475 °C [S cm <sup>-1</sup> ]
			25 °C	500 °C	
LiCl–KCl	58.8-41.2	352 <sup>[81]</sup>	2.01	1.59–1.6 <sup>[82]</sup>	1.69, <sup>[40]</sup> 1.57 (450 °C)
LiI–KI	63.3-36.7	288 <sup>[83]</sup>	3.53	2.77–2.83 <sup>[84]</sup>	1.56, <sup>[40]</sup> 2.24 (607 °C) <sup>[85]</sup>
LiCl–LiI	34.6-65.4	368 <sup>[81]</sup>	3.17	2.57	3.88, <sup>[40]</sup> 3.5 (450 °C)
LiF–LiCl	30.5-69.5	501 <sup>[81]</sup>	2.17	–	–
LiBr–RbBr	42-58	271 <sup>[84]</sup>	3.38	2.63 (647 °C)	1.33 (567 °C) <sup>[38]</sup>
LiCl–KCl–CsCl	57.5-13.3-29.2	265 <sup>[86]</sup>	2.23	–	0.28 (280 °C) <sup>[38]</sup>
LiF–LiCl–LiBr	22-31-47	443 <sup>[87]</sup>	2.91	2.17–2.19 <sup>[82]</sup>	3.21 <sup>[40]</sup>
LiF–LiBr–KBr	2.5-60-37.5	324 <sup>[88]</sup>	3.09	–	1.56 <sup>[40]</sup>
	3-63-34	312 <sup>[88]</sup>	3.12	–	1.75 <sup>[88]</sup>
LiCl–LiBr–KBr	25-37-38	310 <sup>[89,90]</sup>	2.85	–	1.7 <sup>[85]</sup>
LiCl–LiBr–LiI	10.0-16.1-73.9	368	3.40	–	3.68 <sup>[40]</sup>
LiF–LiCl–LiI	11.7-29.1-59.2	341 <sup>[91]</sup>	3.53	2.69 <sup>[82]</sup>	2.77 <sup>[40]</sup>
NaF–NaCl–NaI <sup>[20]</sup>	15-32-53	530	2.90	2.54 (560 °C)	1.7–2.0 (560 °C)
NaCl–KCl–MgCl <sub>2</sub> <sup>[14]</sup>	30-20-50	396	2.10	–	–
LiCl–NaCl–CaCl <sub>2</sub> <sup>[33]</sup>	38-27-35	450	2.14	1.9	2.18
LiCl–NaCl–CaCl <sub>2</sub> –BaCl <sub>2</sub> <sup>[33]</sup>	29-20-35-16	390	2.53	2.24 (600 °C)	1.9 (600 °C)

liquid Na electrode. Na Superionic Conductor (NASICON) is a good Na-ion conductor developed by Goodenough et al. in 1976.<sup>[98]</sup> Na<sub>1+x</sub>Zr<sub>2</sub>Si<sub>x</sub>P<sub>3-x</sub>O<sub>12</sub> (0 ≤ x ≤ 3) was a typical NASICON produced by Ceramtec, Inc (Salt Lake City, Utah), and has been proposed to be used as a solid electrolyte for Na–S batteries.<sup>[99]</sup> Based on the minimal capacity fade of cells with NASICON-type membranes and relatively stable shelf life, NASICON-type materials are considered as promising solid electrolytes for Na–S, ZEBRA and room temperature Na-based batteries. As shown in Figure 19, NASICON-based materials have comparable or even higher Na<sup>+</sup> conductivity than that of β/β′-Al<sub>2</sub>O<sub>3</sub>.

Glass is another type Na<sup>+</sup> conductor, including alkali sulfide glasses (e.g., xLi<sub>2</sub>S–(1-x)P<sub>2</sub>S<sub>5</sub>,<sup>[100]</sup> xNa<sub>2</sub>S–(1-x)P<sub>2</sub>S<sub>5</sub><sup>[101]</sup>), as listed in Figure 19.

### 5.3. Seals and Corrosion

LMEs are usually sensitive to oxygen and moisture at elevated temperature, and exposure of LMEs in air leads to cell degradation, failure and even unsafe issues. So a hermetic seal plays a key role in achieving a long-lasting secondary battery with LEMs. In general, the seals of the cell highly depend on the operating temperature and the chemistry of the cell. At a temperature below 200 °C, polymers can be used for seals and the vapor pressure of liquid metals and electrolyte is minimal. At a higher temperature, to realize a cell with gastight sealing, electrically insulating, chemically stable and thermomechanically robust is a great challenge due to the highly reactive liquid metal vapor pressure, favorable kinetics of reaction between the sealing materials and cell components. At high temperature above 200 °C, almost no polymer can be used for a long-time sealing.

The seals of Na–S and ZEBRA batteries are a sandwich-structure of Al–Al<sub>2</sub>O<sub>3</sub>–Al under a hot-pressing, which boasts a calendar life of over 15 years.<sup>[103]</sup> However, it is difficult to apply the same method and same materials for Li-based LMBs. Unlike the Na, Li can reduce Al<sub>2</sub>O<sub>3</sub> to Al spontaneously, and the sealing fails. Glass and glass-ceramic are another sealing materials for Li–FeS system.<sup>[104,105]</sup> Two issues should be noted: the difference of thermal expansion coefficients between metal (~16 E–6 °C<sup>-1</sup> for SS304) and glass or glass-ceramic (< 10 E–6 °C<sup>-1</sup>), and the relatively low thermal stability of glass and ceramic materials in the cell. Although many studies reported that the thermal expansion coefficients of glass can be adjusted via doping, the thermal stability of the material needs

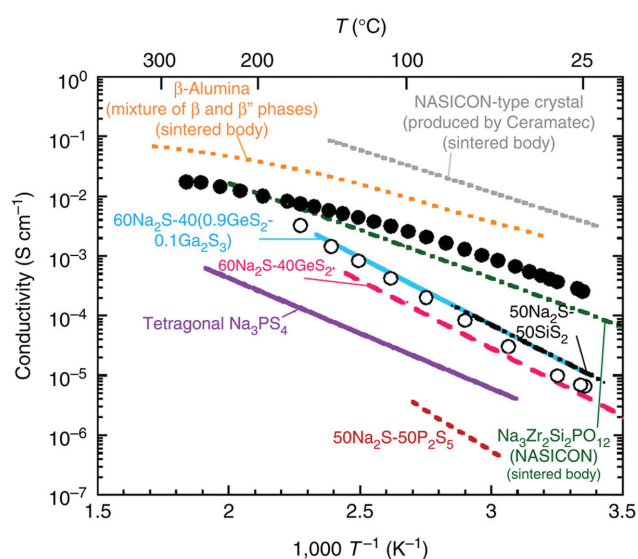


**Figure 19.** Comparison of conductivities of several Na<sup>+</sup> ion conductors. Reproduced with permission.<sup>[102]</sup> Copyright 2012, Nature Publishing Group.

to be further improved.<sup>[106–110]</sup> The commercialization of long-lived, liquid metal batteries rests upon the development of long-lasting, and robust insulating seals.

In addition to seals, high temperature and high-reactive battery materials will undoubtedly induce corrosion and thereby reduce the lifetime of batteries. Corrosion occurs at electrical collectors, cell containers, insulators and seals.<sup>[111,112]</sup> Corrosion can be divided into two categories: chemical corrosion and electrochemical corrosion. In LMBs, highly reactive liquid metals such as Li, Na, etc., can easily react with negative electrode current collectors (alloying), seals and insulating sheath ( $\text{Al}_2\text{O}_3$ ,  $\text{MgO}$ ,  $\text{ZrO}_2$  etc., reduction reaction). Secondly, the corrosion caused by the vapor of liquid negative electrode at high temperature will destroy the seals and insulative components in the cell. On the cathode side, the positive electrode current collector should be compatible with positive electrodes (such as Bi, Pb, Sn and Sb) and the cell container should not dissolve in the liquid positive metal electrodes.<sup>[112]</sup> Furthermore, liquid Na reacting with some solid-state electrolytes in Na-S and ZEBRA is also regarded as corrosion issue.<sup>[113]</sup> Overall, selection of corrosion-resistant secondary battery materials and the technologies on modification of these materials with highly stable coating et al., are very important for commercialization of liquid-electrode-based batteries.

## 6. Conclusion

Liquid metal electrodes are electrically conductive with a soft surface and amorphous structure, which can be facily employed as either anode or cathode in batteries without any complicated manufacturing processes and additives. With the low-cost molten salt electrolyte and liquid metal, as well as the simple electrode manufacturing process, the liquid metal electrode-based batteries are potentially inexpensive for large-scale batteries and hold the promise of achieving the goal of integrating more renewable energy and smoothing fluctuations in the grid in the near future.

In general, the alkaline- and alkaline-earth- metals/alloys act as anodes and the semimetals/alloys are the cathodes for LMBs. During the past several decades, liquid Li and Na negative electrodes based LMBs, Na-S and ZEBRA batteries were intensively researched due to their low melting points, low electronegativity, and easily available electrolytes. Liquid K, Mg and Ca were also investigated as potential electrodes for energy storage batteries. Among these LME-based batteries, Na-S and ZEBRA are relatively mature systems, and LMBs are rapidly developing recently. It is worth noting that the LMB with Li-Sb-Pb chemistry has outstanding cell performance, which potentially meets the metrics for grid energy storage.

However, the liquid metal electrodes only work at elevated temperature higher than the melting point of the metals and/or alloys. The high temperature causes some issues like insulating seals, materials corrosion, thermal management, and the immobility of the cell. More research is necessary on the development of high temperature seals, anti-corrosion and other issues. For LMBs, more efforts should be devoted to developing high-voltage and low-melting liquid metal electrode based batteries through alloying approaches, along with exploring

low-melting-temperature molten salt electrolytes. For Na-beta alumina batteries, enhancing the robustness and simplifying the manufacturing processes of beta-alumina are the key enablers for making Na-beta alumina battery cheaper and more reliable. Furthermore, the development of lower-cost and more earth-abundant multi-valent LMEs, like Mg, Ca and Al, is of great importance for achieving more affordable LME-based batteries for potential large-scale applications.

## Acknowledgments

H.M.L. and H.Y.Y. contributed equally to this work. This work was supported by the Natural Science Foundation of China (Grant 51307069), 973 Program (2015CB258400) and the National Thousand Talents Program of China.

Received: March 2, 2016

Revised: April 8, 2016

Published online: May 31, 2016

- [1] Z. Yang, J. Zhang, M. C. Kintner-Meyer, X. Lu, D. Choi, J. P. Lemmon, J. Liu, *Chem. Rev.* **2011**, *111*, 3577.
- [2] B. Dunn, H. Kamath, J. M. Tarascon, *Science* **2011**, *334*, 928.
- [3] M.-C. Lin, M. Gong, B. Lu, Y. Wu, D.-Y. Wang, M. Guan, M. Angell, C. Chen, J. Yang, B.-J. Hwang, H. Dai, *Nature* **2015**, *520*, 324.
- [4] X. Lu, M. E. Bowden, V. L. Sprenkle, J. Liu, *Adv. Mater.* **2015**, *27*, 5915.
- [5] R. Cao, W. Xu, D. Lv, J. Xiao, J.-G. Zhang, *Adv. Energy Mater.* **2015**, *5*, 1402273.
- [6] M. A. Pope, I. A. Aksay, *Adv. Energy Mater.* **2015**, *5*, 1500124.
- [7] H. Sun, W. Wang, Z. Yu, Y. Yuan, S. Wang, S. Jiao, *Chem. Commun.* **2015**, *51*, 11892.
- [8] S. Okamoto, T. Ichitsubo, T. Kawaguchi, Y. Kumagai, F. Oba, S. Yagi, K. Shimokawa, N. Goto, T. Doi, E. Matsubara, *Adv. Sci.* **2015**, *2*, 1500072.
- [9] K. B. Hueso, M. Armand, T. Rojo, *Energy Environ. Sci.* **2013**, *6*, 734.
- [10] H. Chen, T. N. Cong, W. Yang, C. Tan, Y. Li, Y. Ding, *Prog. Nat. Sci.* **2009**, *19*, 291.
- [11] B. Zakeri, S. Syri, *Renew. Sust. Energy Rev.* **2015**, *42*, 569.
- [12] W. Hoopes, U.S. Patent 1534315, **1925**.
- [13] M. Kondo, H. Maeda, M. Mizuguchi, *M. JOM* **1990**, *42*, 36.
- [14] D. J. Bradwell, H. Kim, A. H. Sirk, D. R. Sadoway, *J. Am. Chem. Soc.* **2012**, *134*, 1895.
- [15] AMBRI Storing Energy for our Future, <http://www.ambri.com/>, (Accessed date: Dec, 2015).
- [16] H. Pan, Y.-S. Hu, L. Chen, *Energy Environ. Sci.* **2013**, *6*, 2338.
- [17] B. L. Ellis, L. F. Nazar, *Curr. Opin. Solid State Mater. Sci.* **2012**, *16*, 168.
- [18] M. Bredig, *Mixtures of Metals with Molten Salts*, Oak Ridge National Lab., Tenn., Oak Ridge, TN **1963**.
- [19] A. Dworkin, H. Bronstein, M. Bredig, *J. Phys. Chem.* **1962**, *66*, 572.
- [20] E. Cairns, C. Crouthamel, A. Fischer, M. Foster, J. Hesson, C. Johnson, H. Shimotake, A. Tevebaugh, Galvanic Cells with Fused-Salt Electrolyte, ANL-7316, Argonne National Lab., Ill., **1967**.
- [21] X. Ning, S. Phadke, B. Chung, H. Yin, P. Burke, D. R. Sadoway, *J. Power Sources* **2015**, *275*, 370.
- [22] W. Weppner, R. Huggins, *J. Electrochem. Soc.* **1978**, *125*, 7.
- [23] K. Wang, K. Jiang, B. Chung, T. Ouchi, P. J. Burke, D. A. Boysen, D. J. Bradwell, H. Kim, U. Muecke, D. R. Sadoway, *Nature* **2014**, *514*, 348.

- [24] M. Bredig, J. Johnson, W. T. Smith Jr., *J. Am. Chem. Soc.* **1955**, *77*, 307.
- [25] M. Bredig, H. Bronstein, *J. Phys. Chem.* **1960**, *64*, 64.
- [26] S. Tamaki, T. Ishiguro, S. Takeda, *J. Phys. F: Metal Physics* **1982**, *12*, 1613.
- [27] H. Shimotake, E. Cairns, presented at Intersociety Energy Conversion Engineering Conference Proceedings, Bimetallic Galvanic Cells with Fused Salt Electrolyte, Miami Beach, FL, USA, Aug. **1967**.
- [28] J. T. Kummer, N. Weber, *SAE Trans.* **1968**, *76*, 1003.
- [29] J. Sudworth, *J. Power Sources* **2001**, *100*, 149.
- [30] J. Johnson, M. Bredig, *J. Phys. Chem.* **1958**, *62*, 604.
- [31] B. Agruss, H. R. Karas, In Regenerative EMF Cells; C. E. Crouthamel, H. L. Recht, Eds.; *Adv. Chem.*, Vol. 64; American Chemical Society: Washington, DC, **1967**, 62.
- [32] A. Dworkin, H. Bronstein, M. Bredig, *Discuss. Faraday Soc.* **1961**, *32*, 188.
- [33] H. Kim, D. A. Boysen, T. Ouchi, D. R. Sadoway, *J. Power Sources* **2013**, *241*, 239.
- [34] T. Ouchi, H. Kim, X. Ning, D. R. Sadoway, *J. Electrochem. Soc.* **2014**, *161*, A1898.
- [35] E. A. Ukshe, N. Bukun, *Russ. Chem. Rev.* **1961**, *30*, 90.
- [36] M. M. Thackeray, C. Wolverton, E. D. Isaacs, *Energy Environ. Sci.* **2012**, *5*, 7854.
- [37] Y. Lu, Z. Tu, L. A. Archer, *Nat. Mater.* **2014**, *13*, 961.
- [38] P. Masset, R. A. Guidotti, *J. Power Sources* **2007**, *164*, 397.
- [39] R. A. Guidotti, P. J. Masset, *J. Power Sources* **2008**, *183*, 388.
- [40] P. Masset, A. Henry, J.-Y. Poinso, J.-C. Pogniet, *J. Power Sources* **2006**, *160*, 752.
- [41] T. Kaun, P. Nelson, L. Redey, D. Vissers, G. Henriksen, *Electrochim. Acta* **1993**, *38*, 1269.
- [42] G. Henriksen, D. Vissers, *J. Power Sources* **1994**, *51*, 115.
- [43] J. Songster, A. Pelton, *J. Phase Equilib.* **1992**, *13*, 300.
- [44] H. Shimotake, G. Rogers, E. Cairns, *Ind. Eng. Chem. Proc. Des. Dev.* **1969**, *8*, 51.
- [45] M. R. Gao, Y. F. Xu, J. Jiang, S. H. Yu, *Chem. Soc. Rev.* **2013**, *42*, 2986.
- [46] S. Poizeau, H. Kim, J. M. Newhouse, B. L. Spatocco, D. R. Sadoway, *Electrochim. Acta* **2012**, *76*, 8.
- [47] C. J. Wen, R. A. Huggins, *J. Electrochem. Soc.* **1981**, *128*, 1181.
- [48] M. L. Saboungi, J. Marr, M. Blander, *J. Chem. Phys.* **1978**, *68*, 1375.
- [49] S. Zachary, Clean Technica, <http://cleantechnica.com/2014/10/13/ambri-ceo-interview-phil-giudice/>, Oct. 2015.
- [50] M. D. Slater, D. Kim, E. Lee, C. S. Johnson, *Adv. Funct. Mater.* **2013**, *23*, 947.
- [51] S. W. Kim, D. H. Seo, X. Ma, G. Ceder, K. Kang, *Adv. Energy Mater.* **2012**, *2*, 710.
- [52] N. Yabuuchi, K. Kubota, M. Dahbi, S. Komaba, *Chem. Rev.* **2014**, *114*, 11636.
- [53] S. Matsunaga, T. Ishiguro, S. Tamaki, *J. Phys. F: Metal Phys.* **1983**, *13*, 587.
- [54] F. Neale, N. Cusack, *J. Phys. F: Metal Phys.* **1982**, *12*, 2839.
- [55] R. D. Weaver, S. W. Smith, N. L. Willmann, *J. Electrochem. Soc.* **1962**, *109*, 653.
- [56] B. Agruss, *J. Electrochem. Soc.* **1963**, *110*, 1097.
- [57] H. Kim, D. A. Boysen, J. M. Newhouse, B. L. Spatocco, B. Chung, P. J. Burke, D. J. Bradwell, K. Jiang, A. A. Tomaszowska, K. Wang, W. Wei, L. A. Ortiz, S. A. Barriga, S. M. Poizeau, D. R. Sadoway, *Chem. Rev.* **2013**, *113*, 2075.
- [58] E. Cairns, E. Gay, R. Steunenber, H. Shimotake, J. Selman, T. Wilson, D. Webster, *Development of High Specific Energy Batteries for Electric Vehicles*, ANL-7593; Argonne National Lab: Chicago **1972**, 1.
- [59] E. C. Gay, J. D. Arntzen, E. J. Cairns, J. Kincinas, J. Riha, L. Trevor, W. J. Walsh, D. S. Webster, *Lithium Chalcogen Secondary Cells for Components in Electric Vehicular Propulsion Generating Systems*, ANL-7863; Argonne National Laboratory: Chicago **1972**.
- [60] J. Hesson, M. Foster, H. Shimotake, *J. Electrochem. Soc.* **1968**, *115*, 787.
- [61] J. Coetzer, *J. Power Sources* **1986**, *18*, 377.
- [62] X. Lu, G. Xia, J. P. Lemmon, Z. Yang, *J. Power Sources* **2010**, *195*, 2431.
- [63] T. Oshima, M. Kajita, A. Okuno, *Int. J. Appl. Ceram. Technol.* **2004**, *1*, 269.
- [64] D. Rastler, *Electrical Energy Storage Technology Options, Report 1020676*, Electric Power Research Institute, Palo Alto, CA, Dec. **2010**.
- [65] M. Hosseinifar, A. Petric, *J. Power Sources* **2012**, *206*, 402.
- [66] X. Lu, G. Li, J. Y. Kim, J. P. Lemmon, V. L. Sprenkle, Z. Yang, *J. Power Sources* **2012**, *215*, 288.
- [67] A. V. Virkar, L. Viswanathan, D. R. Biswas, *J. Mater. Sci.* **1980**, *15*, 302.
- [68] L. Viswanathan, A. V. Virkar, *J. Mater. Sci.* **1982**, *17*, 753.
- [69] M. W. Breiter, B. Dunn, R. W. Powers, *Electrochim. Acta* **1980**, *25*, 613.
- [70] J. L. Sudworth, A. Tilley, *The Sodium Sulfur Battery*, Kluwer Academic Pub, Chapman Hall, London, UK **1985**.
- [71] W. G. Bugden, P. Barrow, J. H. Duncan, *Solid State Ionics* **1981**, *5*, 275.
- [72] D. Reed, G. Coffey, E. Mast, N. Canfield, J. Mansurov, X. Lu, V. Sprenkle, *J. Power Sources* **2013**, *227*, 94.
- [73] X. Lu, G. Li, J. Y. Kim, D. Mei, J. P. Lemmon, V. L. Sprenkle, J. Liu, *Nat. Commun.* **2014**, *5*, 4578.
- [74] A. Ignaszak, P. Pasierb, R. Gajerski, S. Komornicki, *Thermochim. Acta* **2005**, *426*, 7.
- [75] R. P. Clark, K. R. Grothaus, *J. Electrochem. Soc.* **1971**, *118*, 1680.
- [76] H. Kim, D. A. Boysen, D. J. Bradwell, B. Chung, K. Jiang, A. A. Tomaszowska, K. Wang, W. Wei, D. R. Sadoway, *Electrochim. Acta* **2012**, *60*, 154.
- [77] A. Bhatia, W. Hargrove, *Phys. Rev. B* **1974**, *10*, 3186.
- [78] D. P. Tao, *Thermochim. Acta* **2000**, *363*, 105.
- [79] J. M. Newhouse, S. Poizeau, H. Kim, B. L. Spatocco, D. R. Sadoway, *Electrochim. Acta* **2013**, *91*, 293.
- [80] T. Ouchi, H. Kim, B. L. Spatocco, D. R. Sadoway, *Nat. Commun.* **2016**, *7*, DOI: 10.1038/ncomms10999.
- [81] J. Sangster, A. D. Pelton, *J. Phys. Chem. Ref. Data* **1987**, *16*, 509.
- [82] P. Masset, S. Schoeffert, J.-Y. Poinso, J.-C. Pogniet, *J. Power Sources* **2005**, *139*, 356.
- [83] R. Sridhar, C. E. Johnson, E. J. Cairns, *J. Chem. Eng. Data* **1970**, *15*, 244.
- [84] G. Janz, R. Tomkins, C. Allen, J. Downey Jr, S. Singer, *J. Phys. Chem. Ref. Data* **1977**, *6*, 409.
- [85] G. J. Janz, *NIST Standard Reference Database 27: Properties of Molten Salts Database. Single Salts and Salt Mixtures Data; Density, Viscosity, Electrical Conductance, and Surface Tension*, Ver. 20, **1992**.
- [86] E. Cairns, R. Steunenber, High-Temperature Batteries, in: C. Rouse (Ed.), *Progress in High Temperature Physics and Chemistry*, Pergamon Press, New York, **1973**, p63.
- [87] A. Bergman, A. Arabadshian, *Russ. J. Inorg. Chem. (English Trans.)* **1963**, *8*, 369.
- [88] P. Masset, *J. Power Sources* **2006**, *160*, 688.
- [89] T. D. Kaun, *J. Electrochem. Soc.* **1985**, *132*, 3063.
- [90] D. Vissers, L. Redey, T. Kaun, *J. Power Sources* **1989**, *26*, 37.
- [91] C. E. Johnson, E. J. Hathaway, *J. Chem. Eng. Data* **1969**, *14*, 174.
- [92] X. Wei, Y. Cao, L. Lu, H. Yang, X. Shen, *J. Alloys Compd.* **2011**, *509*, 6222.
- [93] S. Sartori, A. Martucci, A. Muffato, M. Guglielmi, *J. Eur. Ceram. Soc.* **2004**, *24*, 911.

- [94] Z. Wang, X. Li, Z. Feng, *Bull. Korean Chem. Soc.* **2011**, *32*, 1311.
- [95] J. D. Hodge, *Am. Ceram. Soc. Bull.* **1983**, *62*, 244.
- [96] A. Pekarsky, P. S. Nicholson, *Mater. Res. Bull.* **1980**, *15*, 1517.
- [97] H. C. Park, Y. B. Lee, S. G. Lee, C. H. Lee, J. K. Kim, S. S. Hong, S. S. Park, *Ceram. Int.* **2005**, *31*, 293.
- [98] J. Goodenough, H.-P. Hong, J. Kafalas, *Mater. Res. Bull.* **1976**, *11*, 203.
- [99] E. R. Losilla, M. A. Aranda, S. Bruque, J. Sanz, M. A. Paris, J. Campo, A. R. West, *Chem. Mater.* **2000**, *12*, 2134.
- [100] M. Yang, J. Hou, *Membranes* **2012**, *2*, 367.
- [101] S. S. Berbano, I. Seo, C. M. Bischoff, K. E. Schuller, S. W. Martin, *J. Non-Cryst. Solids* **2012**, *358*, 93.
- [102] A. Hayashi, K. Noi, A. Sakuda, M. Tatsumisago, *Nat. Commun.* **2012**, *3*, 856.
- [103] M. Nicholas, R. Crispin, *J. Mater. Sci.* **1982**, *17*, 3347.
- [104] N. PA, D. Barney, R. Steunenberg, A. Chilenskas, E. Gay, J. Battles, F. Hornstra, W. Miller, M. Roche, H. Shimotake, R. Hudson, R. Rubischko, S. Sudar, *High-Performance Batteries for Electric-Vehicle Propulsion and Stationary Energy Storage*, ANL-78-94, Argonne National Laboratory, Argone Ill. **1978**.
- [105] S. Song, Z. Wen, Y. Liu, J. Lin, X. Xu, Q. Zhang, *J. Solid State Electrochem.* **2010**, *14*, 1735.
- [106] S.-B. Sohn, S.-Y. Choi, G.-H. Kim, H.-S. Song, G.-D. Kim, *J. Non-Cryst. Solids* **2002**, *297*, 103.
- [107] S. B. Sohn, S. Y. Choi, G. H. Kim, H. S. Song, G. D. Kim, *J. Am. Ceram. Soc.* **2004**, *87*, 254.
- [108] J. W. Fergus, *J. Power Sources* **2005**, *147*, 46.
- [109] S. T. Reis, R. K. Brow, *J. Mater. Eng. Perform.* **2006**, *15*, 410.
- [110] M. K. Mahapatra, K. Lu, *Mater. Sci. Eng.: R: Rep.* **2010**, *67*, 65.
- [111] G. J. Janz, R. P. Tomkins, *Corrosion.* **1979**, *35*, 485.
- [112] R. N. Lyon, *Liquid-Metals Handbook*, US Government Printing Office, Washington DC **1952**.
- [113] O. Bohnke, S. Ronchetti, D. Mazza, *Solid State Ionics* **1999**, *122*, 127.